# The Map3k12 (Dlk)/ JNK3 signaling pathway is required for pancreatic beta-cell proliferation during postnatal development

**Mathie Tenenbaum[1], Valérie Plaisance[1,2], Raphael Boutry[1], Valérie Pawlowski[1,2], Cécile Jacovetti[3], Clara Sanchez-Parra[3], Hélène Ezanno[1], Julien Bourry[1], Nicole Beeler[1], Gianni Pasquetti[4], Valery Gmyr[4], Stéphane Dalle[5], Julie Kerr-Conte[4], François Pattou[4], Syu-ichi Hirai[6], Romano Regazzi[3], Amélie Bonnefond[1,7], Philippe Froguel[1,7] and Amar Abderrahmani[1,2,7]**

[1]Univ. Lille, CNRS, Institut Pasteur de Lille, UMR 8199 - EGID, F-59000 Lille, France

[2]Univ. Lille, CNRS, Centrale Lille, ISEN, Univ. Valenciennes, UMR 8520, IEMN, F-59000 Lille, France

[3]Department of Fundamental Neuroscience, University of Lausanne, Switzerland

[4]Univ. Lille, Inserm, CHU Lille, U1190 - EGID, F-59000 Lille, France

[5]Institut de Génomique Fonctionnelle, CNRS UMR5203, INSERM U1191, Montpellier University, Montpellier, France

[6]Département of Biology, Wakayama University, Japan

[7]Department of Medicine, Section of Genomics of Common Disease, Imperial College London, UK

Correspondence to:

mathie.tenenbaum@univ-lille.fr and amar.abderrahmani@univ-lille.fr

**Abstract**

Unveiling the key pathways underlying postnatal beta-cell proliferation can be instrumental to decipher the mechanisms of beta-cell mass plasticity to increased physiological demand of insulin during weight gain and pregnancy. Using transcriptome and global Serine Threonine Kinase activity (STK) analyses of islets from newborn (10 days old) and adult rats, we found that highly proliferative neonatal rat islet cells display a substantially elevated activity of the mitogen activated protein 3 kinase 12, also called dual leucine zipper-bearing kinase (Dlk). As a key upstream component of the c-Jun amino terminal kinase (Jnk) pathway, Dlk overexpression was associated with increased Jnk3 activity and was mainly localized in the beta-cell cytoplasm. We provide the evidence that Dlk associates with and activates Jnk3, and that this cascade stimulates the expression of *Ccnd1* and *Ccnd2*, two essentials cyclins controlling postnatal beta-cell replication. Silencing of *Dlk* or of *Jnk3* in neonatal islet cells dramatically hampered primary beta-cell replication and the expression of the two cyclins. Moreover, the expression of *Dlk*, *Jnk3*, *Ccnd1* and *Ccnd2* was induced in high replicative islet beta-cells from *ob/ob* mice during weight gain, and from pregnant female rats. In human islets from non-diabetic obese individuals, DLK expression was also cytoplasmic and the rise of the mRNA level was associated with an increase of *JNK3, CCND1 and CCND2* mRNA levels, when compared to islets from lean and obese patients with diabetes. In conclusion, we find that activation of Jnk3 signalling by Dlk could be a key mechanism for adapting islet beta-cell mass during postnatal development and weight gain.

**Keywords:** Beta-cell mass; Mapk; Obesity; pregnancy; postnatal development

**Abbreviations:**

**Ccnd:** Cyclin D

**Cdk:** Cyclin-dependent kinase

**Cdkn:** Cyclin-dependent kinase inhibitor

**DLK:** Dual leucine Zipper Kinase

**JNK:** c-Jun amino terminal kinase

**MAP3K12:** Mitogen-activated protein kinase kinase kinase 12

**MAPK10:** Mitogen-activated protein kinase 10

**STK:** Serine threonine kinase

**Introduction**

Pancreatic beta-cell mass expansion is fundamental for achieving appropriate glucose control in response to physiological and pathophysiological conditions [1]. In rodent models of obesity and pregnancy, the expansion of the functional beta-cell mass relies mainly on increased beta-cell proliferation [2, 3]. Although proliferation of human islet cells is still debated, there is some evidence for an increase in pancreatic beta-cell replication in obese individuals [4, 5]. During the postnatal development, the elevated replication rate of pancreatic beta-cells that precedes the acquisition of glucose competence is a key process permitting the necessary expansion of the beta-cell mass [6]. In rats, beta-cell replication is substantial from birth until the $10^{th}$ postnatal day [7]. Thereafter, the replication rate decreases overtime and remains more or less constant throughout the adult life [7]. In human, a similar pattern of beta-cell growth associated with postnatal beta-cell mass expansion has been postulated [8, 9]. The greatest beta-cell replication is observed before 2 years of age with a progressive decline continuing until 5 years [8, 9]. Therefore, the postnatal proliferative capacity is critical for achieving an appropriate adult beta-cell mass, which is important for preventing type 2 diabetes development.

Several independent studies have reported that stimulation of cell cycle gene expression cyclin D2 (*Ccnd2*) and D1 (*Ccnd1)* regulating the cyclin dependent kinases 4 and 6 is a key for postnatal beta-cell growth [7, 10]. The upstream regulation of the two cyclins usually rely on serine threonine kinases (STKs) activation, a group of enzymes comprising hundreds of members including mitogen activated protein kinases (MAPKs) [11]. The c-Jun N terminal kinases (Jnks) group of the MAPKs driven by the Map3k12 also called Dual leucine Zipper Kinase (Dlk) regulates cell proliferation in a mechanism evolving the stimulation of Ccnd1 [12]. In pancreatic beta cells, several STKs have been identified as key players in the regulation of both proliferation and mass in response to physiological and pathophysiological conditions in adults [13]. Some of them are therapeutic targets of the Glucagon-like peptide 1 (GLP-1) receptor agonists, current antidiabetic medicines that potentiate glucose-induced insulin secretion, stimulate beta-cell proliferation and protect beta cell against apoptosis [14]. The identification of STK regulating *Ccnd2* and *Ccnd1* and thereby beta-cell proliferation during postnatal development would be insightful for identifying new targets for improving beta-cell mass in diabetes. In the present study, using transcriptome analysis and whole STK activity measurement, we found that Map3k12 (Dlk)/ Mapk10 (Jnk3) signaling is stimulated in neonate islets and is required for postnatal beta-cell mass proliferation and expansion by inducing *Ccnd2* and *Ccnd1*. In addition, we found that this signaling is likely involved in beta-cell mass adaptation in response to weight gain and pregnancy.

**Materials and Methods**

***Animals***. Male and pregnant female Sprague–Dawley rats were obtained from Janvier Laboratories (Le Genest-Saint-Isle, France) and housed under a 12 h/12 h light/dark cycle in a climate-controlled and pathogen-free facility. All procedures were performed in accordance with the Guide for the Care and Use of Laboratory Animals from the National Institutes of Health and were approved by the local committee and Veterinary Office. At birth, litters were adjusted to 10-12 pups per dam to standardise the mothers' milk availability. Newborn males and females were nursed until they were euthanised at postnatal day (P)10. Control female mice and obese (*ob*/*ob*) female mice of the C57BL/6J background were obtained from Elevage Janvier (Le Genest-Saint-Isle, France).

***Cell culture.*** Rat pancreatic islets were isolated by collagenase digestion and then purified on a Histopaque density gradient. Islets were dissociated by trypsinization in Trypsin-EDTA 0,5 % (Thermofisher) at 37°C for 8 min. The insulin-secreting cell line (INS-1E) and dispersed rat islet cells were maintained as previously described [7]. Isolated human islets were obtained from the biotherapies for diabetes unit from the «Centre Hospitalier Régional et Universitaire de Lille». Human pancreases were harvested from adult brain-dead donors in accordance with French regulations and with the local Institutional Ethical Committee from the «Centre Hospitalier Régional et Universitaire de Lille». Isolation and preparation of islets in Lille were conducted as described previously [15].

***Western Blotting***. Cells were incubated for 30 minutes on ice in the lysis buffer (20 mM Tris acetate, 0.27 mM Sucrose, 1% Triton X-100, 1 mM EDTA, 1 mM EGTA, 50 mM Sodium Fluoride, 10 mM BetaGlycérophosphate, 1 mM DTT) supplemented with proteases and phosphatases inhibitors (Roche). For nuclear extracts preparation, the cells were scraped into 1.5 ml of cold phosphate-buffered saline (PBS), pelleted for 10 seconds and resuspended in 400 µl cold Buffer A (10 mM HEPES-KOH pH 7.9 at 4°C, 1.5 mm MgCl2, 10 mM KC1, 0.5 mM dithiothreitol, 0.2 mM PMSF) by flicking the tube. The cells were allowed to swell on ice for 10 minutes, and then vortexed for 10 seconds. Samples were centrifuged for 10 seconds, and the supernatant fraction discarded. The pellet was resuspended in 20-100 µl (according to the starting number of cells) of cold Buffer C (20 mM HEPES-KOH pH 7.9, 25% glycerol, 420 mM NaCl,1.5 mM MgCl2, 0.2 mM EDTA, 0.5 mM dithiothreitol, 0.2mM PMSF) and incubated on ice for 20 min for high-salt extraction. Cellular debris were removed by centrifugation for 2 minutes at 4°C and the supernatant (containing nuclear proteins) was stored at -70°C. For Western blotting experiments, total protein extract was separated on 10% SDS-Polyacrylamide gel and electrically blotted to nitrocellulose membrane. The proteins were detected after an overnight incubation of the membrane at 4°C with the specific primary antibodies (all the antibodies are listed in the **table S1**). Proteins were visualized with IRDye800 or IRDye700 (Rockland Immochemicals) as secondary antibodies. Quantification was performed using the Odyssey Infrared Imaging System (Rockland Immochemicals) or ImageJ software.

***Immunofluorescence.*** 10 days old and adult rats were killed, and their pancreases were harvested, fixed in 4% formaldehyde, and processed for paraffin embedding and preparation of 10-µm sections. Beta and alpha cells were visualized by insulin staining using guinea pig anti-insulin antibody (1:100, Dako) and mouse anti-glucagon (1:100, Sigma), respectively. Dlk was detected using the rabbit anti-Dlk primary antibody (1:1000; Genetex) in PBST supplemented with 3% BSA at 4°C overnight. After being rinsed three times for 10 min each in PBST, slides were

incubated with secondary antibody Alexa Fluor (1:500 diluted in PBST plus 1% BSA, Thermofisher) at room temperature for 1 h and were then thoroughly rinsed again. The slides were mounted using a mounting kit containing DAPI (Vectashield. Eurobio-Ingen, H-1200). Cells were observed under a fluorescence microscope. For immunofluorescence of insulin, glucagon and Dlk, whole embryos of littermates control C57BL/6N and KO mice (resulting from the LacZ replacement of the coding exons 1, 2, and a part of 3 of the *Map3K12* gene in C57BL/6N mouse) were fixed overnight in 4% paraformaldehyde (PFA) at 4°C and embedded in paraffin as previously described [16]. Fluorescence images were taken under an Olympus BX51 microscope equipped with DP70 digital camera and the DPManager (DPController) software.

***Immunoprecipitation (IP).*** INS-1E cells were transfected with the plasmid coding for Dlk cDNA (pcDlk) or small interfering RNA directed against Dlk (siDlk) using Lipofectamime 2000 (Invitrogen) as described [17]. 48 h after transfection, cells were washed with cold PBS and were lysed in 20 mM Tris pH 7.5, 150 mM NaCl 0.1% Triton X-100 buffer (plus protease and phosphatase inhibitors) for 30 min at 4°C. After centrifugation, the amount of proteins was quantified using bicinchoninic acid protein assay (BCA) reagent (Thermo Fisher Scientific). 500 µg of proteins were then immunoprecipitated with anti-Dlk (1/1000; Genetex) or anti-Jnk3 (1/1000, Cell Signaling) antibodies that have been pre-coupled to protein G Sepharose (GE Healthcare). Proteins were eluted with SDS sample buffer and subjected to SDS/PAGE and subsequent immunoblotting. Approximately 5% of the protein was run as input, whereas 30% of the pull-down was run in each lane of the Western blots and blotted with anti-Dlk or anti-Jnk3 antibodies.

***Apoptosis and proliferation***. Dispersed rat islet cells were seeded on poly-L-lysine–coated glass coverslips. After the treatment, the coverslips were washed with PBS and the cells were fixed with methanol. For measuring proliferation with BrdU, the cells were incubated with BrdU (Sigma) 10 µM for 24h. After permeabilization in PBS-saponin solution, non-specific binding were blocked in a solution of PBS-saponin containing 1% BSA. The cells were then incubated with primary antibodies for 1 h (Ki67, BrdU, Insulin, Glucagon) followed by exposure to secondary antibodies. Coverslips were mounted using a mounting kit containing DAPI (Vectashiled. Eurobio-Ingen, H-1200) and images were analysed with axioscan, an immune slide automatized scanner. Apoptosis was measured by TUNEL assays according to manufacturer's protocol (R&D systems).

***Insulin secretion***. Dissociated rat islet cells were preincubated with KREBS buffer (127 mM NaCl, 4.7 mM KCl, 1 mM CaCl2, 1.2 mM KH2PO4, 1.2 mM MgSO4, 25 mM HEPES, 5 mM NaHCO3) containing 2 mM glucose (basal condition) during 30 min at 37 C. The medium was then replaced by either the same buffer (basal condition) or a KREBS buffer supplemented with 20 mM of glucose (stimulatory condition). After 45 min, the supernatants were collected and cellular insulin contents were recovered in EtOH acid (75% EtOH, 1.5% HCl). The amount of insulin in the samples was determined by ELISA (Mercodia).

***Transfection***. INS-1E and dispersed rat islet cells were transfected with small interfering RNA directed against Dlk (siDLK) or JNK3 (siJNK3) using Lipofectamime RNAimax (Thermofisher) as described in [17]. The *Map3k12 (Dlk)* and MAPK10 (Jnk3) mRNA target sequences were 5'-AUA CGA CGA UGU GGU GAA GAU CUC dTdT-3' and 5' AGC GGA UGU ACU AGC UTT-3', respectively.

***Quantitative PCR.*** Total RNA was extracted using Aurum Total RNA Mini Kit (Bio-Rad) according to the manufacturer's protocol. Total RNA was collected from the pools of pancreatic islets of Postnatal day 1 (P1, four pups), P5 (four pups) and P10 (two pups), while in P15, P20, P23, P31 and adult rats, total RNA was extracted from islets of individual animal. The reverse transcription reaction was performed as previously described [18]. Real-time quantitative-PCR assays were carried out on the Bio-Rad MyiQ Real-Time PCR Detection System using iQ SyBr Green Supermix (Bio-Rad) as previously described [18]. The primer sequences used are: *Ccnd1* (sense 5′-AGCAGAAGTGCGAAGAGGAG-3' and antisense 5'- -GAGCTTGTTCACCAGAAGCA-3'); *Rplp0* (sense 5'-ACCTCCTTCTTCCAGGCTTT-*3'* and antisense *5'*-CCTCTTTCTTCCAAGCTTT-3'); *Tbp* (sense 5′-CGTGCCAGAAATGCTGAATA-3' and antisense 5'- CTGGTGGGTCAACACAAGG -3'); *Mapk10 (Jnk3)* (sense *5'*-CGTGGACATATGGTCTGTGG-3' and antisense 5'-AGGTGAGGCCTGCATACTTG-3'); *Map3k12 (Dlk)* (sense *5'*-TTAAATCCCAGGCAGAGTGG-3' and antisense 5'-GAGGGCATTCAGTTCCATGT-3'); *Ccnd2* (sense *5'*-GACTGCGGAAAAGCTGTGTA-3' and antisense 5'-TGCTCAATGAAGTCGTGAGG-3')

***PamChip peptide microarrays for kinome analysis.*** See supplementary methods.

***Statistical analyses***. The experiments including more than two groups were analyzed by ANOVA or with the non-parametric equivalent Kruskal-Wallis test followed by post-hoc Bonferroni test (Dunnett's test) when experiments included more than 2 groups.

**RESULTS**

***Map3k12 (Dlk) expression is involved in beta-cell proliferation during the postnatal development of newborn rats.*** We previously identified through transcriptome analysis a 70-fold higher expression of *Map3k12* in pancreatic islets of 10 days old rats compared to those of adult animals [7]. *Map3k12* encodes the mitogen activated protein 3 kinase 12, a STK also called dual leucine zipper-bearing kinase (Dlk). The expression changes of *Map3k12* (*Dlk*) during the postnatal period was further studied by quantitative PCR and Western Blotting experiments. We found a 2-4 folds increase of the *Map3k12* (*Dlk*) expression between p1 and p10 postnatal days, and declines thereafter, suggesting a transient postnatal activation (**Fig. 1a and 1b**). Map3k12 (Dlk) has a multitude of roles that rely on the cellular and environmental context, which may even appear paradoxical. In beta cells, Map3k12 (Dlk) plays a dual role according to its subcellular localization [19]. While the presence of Map3k12 (Dlk) in the nucleus is associated with beta-cell death, the cytosolic localization of the kinase drives opposite cell outcome [19]. In addition, plasmid-based overexpression of Dlk has been associated with increased apoptosis in immortalized insulin-producing cells including HIT cells [19] and INS-1 cells (**Fig. S1a and S1b**). Therefore, we investigated the subcellular localization of overexpressed Map3k12 (Dlk) in islets of 10 days old rats. Immunofluorescence (IF) and Western Blotting experiments showed that Map3k12 (Dlk) overexpression is enriched in the cytosol fraction of isolated islet cells of neonate rats (**Fig. 1c-i**). The cytosolic localization of the kinase observed in islet cells from adult rats (**Fig. S2**), suggests that overexpression of *Map3k12* (*Dlk*) is not associated with a potential change in the nuclear-cytoplasmic distribution of the protein during postnatal development. As beta-cells of neonate rats are highly replicative and have immature glucose-responsiveness [7], we hypothesized that the transient overexpression of *Map3k12* (*Dlk*) plays a role for beta-cell replication.

To assess a possible involvement of the kinase in beta-cell mass expansion, we measured the proliferation rates of dispersed islet cells from 10 days old rats in which the expression of *Map3k12* (*Dlk*) was reduced using small interfering RNAs (**Fig. 2a**). *Map3k12* (*Dlk*) silencing resulted in a marked reduction in beta-cell proliferation, as monitored by ki67 or BrdU and insulin co-staining (**Fig. 2b-c and Fig. S3)**. The loss of beta-cell proliferation by *Map3k12* (*Dlk*) silencing was associated with the drop of *Ccnd2* and *Ccnd1* mRNA levels (**Fig. 2d**). Decreased beta-cell proliferation by siDlk was not associated with a change in beta-cell apoptosis (**Fig. 2e and Fig. S4**) and insulin secretion (**Fig. 2f**). Moreover, the expression of key beta-cell genes including *Glut2, Pdx1, MafA, Ins2, GCK, Znt8, Kir6.2* and *Nkx6.1* were unaltered by *Map3k12* (*Dlk*) silencing (**Fig. S5**), confirming that the kinase is not involved for specialized beta-cell function. Taken together, our data support the hypothesis that increased *Map3k12* (*Dlk*) expression is required for beta-cell proliferation during postnatal development in a mechanism involving Ccnd2 and Ccnd1.

Map3k12 (Dlk) is a strong activator of Mapk signaling including c-Jun amino terminal kinases (Jnk) in different cell types [19, 20], suggesting that Mapk/Jnk activity links Map3k12 (Dlk) to beta-cell proliferation in islets of 10 days old rats. In support of this hypothesis, the measurement of the phosphorylation of hundreds of validated STK substrates by Pamgene technology [18] confirmed the increased activity of the three Mapks/Jnks, including Mapk8 (Jnk1), Mapk9 (Jnk2) and Mapk10 (Jnk3) among the 25 STKs activity that are stimulated in islets of 10 days old rats when compared to adult rats (**Fig. S6**). Increased Mapks/Jnk activity was associated with Mapks/Jnks activation as shown by Western blotting using antibodies recognizing the phosphorylated forms of the three Jnk isoforms (**Fig. 3a-b**). However, in beta-cells, Mapk10 (Jnk3) triggers antiapoptotic and trophic effects, whereas Mapk8

(Jnk1) and Mapk9 (Jnk2) are pro-apoptotic [21]. While they are antagonists, the three Mapks were released from the kinome analysis, because they phosphorylate similar peptide targets. Therefore, we suggested that only Mapk10 (Jnk3) activation couples the effect of Map3k12 (Dlk) to beta-cell proliferation in neonate islets. Several lines of evidences support this hypothesis. First, in agreement with previous data [7], basal beta-cell apoptosis is similar between 10 days old and adult rats (**Fig. S7**). Second, Jnk1 and Jnk2 phosphorylation at functional Thr183/ Tyr185 residues was not induced in islet cells from 10 days old when compared to adult rats (**Fig. 3c-d**). So, we hypothesized that Map3k12 (Dlk) overexpression directly leads to Mapk10 (Jnk3) activation. In addition, we postulated that the mechanism does not rely on the changes in the expression of Mapk10 (Jnk3) as the Mapk10 (Jnk3) mRNA level was similar in islets of 10 old days and adult rats (**Fig. 3e**). To assess the regulation of Mapk10 (Jnk3) by Map3k12 (Dlk), we performed coimmunoprecipitation experiments using the rat INS-1E as unlimited beta-cells source mimicking beta cells of neonate rats. As previously shown in HIT cells [22], Map3k12 (Dlk) regulates Mapk/Jnk activation in INS-1E cells (**Fig. S8**). Immunoprecipitation experiments confirmed that Map3k12 (Dlk) associates with Mapk10 (Jnk3) in INS-1E cells (**Fig.3f**). Association of Dlk and Jnk3 was further validated by immunoprecipitation of Dlk and Jnk3 in HeLa that overexpressed both proteins (**Fig. S9**). Moreover, as expected, silencing or overexpression of Dlk modulated the phosphorylation of Mapk10 (Jnk3) in INS-1E cells (**Fig. 3g and 3h**). All these results indicate that Map3k12 (Dlk) activates Mapk10 (Jnk3) in beta cells.

Silencing of Mapk10 (Jnk3) in islets of 10 days old rats reduced beta-cell proliferation as monitored by Ki67 and BrdU (**Fig. 4a-c and Fig. S10**), suggesting that Mapk10 (Jnk3) activation by Map3k12 (Dlk) accounts for beta-cell proliferation during postnatal development. Moreover, the diminished beta-cell proliferation caused by Mapk10 (Jnk3) silencing was associated with the reduction of *Ccnd2* and *Ccnd1* mRNA (**Fig. 4d**). These results indicate that the Map3k12 (Dlk) / Mapk10 (Jnk3) signaling are required for beta-cell proliferation by controlling the expression of *Ccnd2* and *Ccnd1*.

***Map3k12 expression is increased in islet cells in response to weight gain and pregnancy conditions***

Induction of Map3k12 (Dlk) in highly proliferative beta cells suggests that Map3k12 (Dlk) signaling contributes to beta-cell mass expansion during body growth and development. To verify this hypothesis, we analysed embryos of Dlk-Knockout (KO), in which the Mapk (Jnk) activity including Mapk10 (Jnk3) is totally impaired [16]. Although the homozygous mutant animals (KO) survived during embryonic stages without showing any gross tissue abnormality, they died perinatally, and no KO mutant survived until weaning [16]. Dlk gene disruption results in abnormalities in brain development that are characterized by major defects in axon growth and radial migration of neocortical pyramidal neurons [16]. Besides brain development abnormalities, we observed that beta-cell mass in the KO embryos was reduced (**Fig. S11)**. To further gain insights into the contribution of Map3k12 (Dlk) in the beta-cell expansion, we next measured its expression in insulin-secreting cells from rodent models of pregnancy and obesity. We first measured the expression of *Map3k12 (Dlk), Ccnd1* and *Ccnd2* in islet cells from pregnant rats at 14 days of gestation that display increased beta-cell replication [23]. In pregnant rats, it was previously shown that the islet beta-cell replication increases after 10 days of gestation (G10), peaks at 14 days (G14), and decreases thereafter until delivery [3, 24]. We found that the expression of *Map3k12 (Dlk), Mapk10* (*Jnk3*), *Ccnd1* and *Ccnd2* raises compared to age-matched non-pregnant female rats starting from G10 and reaches its maximum at G14 (**Fig. 5a**). As expected from beta-cell replication studies [3, 24], the expression of the three mRNA level decreased after G14 (**Fig. 5a**).

In obesity rodent models, such as *ob/ob*, the beta-cell proliferation largely contributes to the expansion of the beta-cell mass and rises in response to insulin resistance [2, 25]. In *ob/ob* mice, islet beta-cell growth is prominent in 5 to 8 weeks old animals [26]. We found that the expression of *Map3k12 (Dlk)* is increased in 5 and 8 weeks-old *ob/ob* mice compared to controls mice (**Fig. 5b**). The subcellular localization of Map3k12 (Dlk) in islets of 8 weeks old ob/ob and age-matched control mice were similar, supporting a role for Map3k12 (Dlk) in the beta-cell proliferation during weight gain (**Fig. S12**). Moreover, induction of *Map3k12 (Dlk)* in 5 and 8 weeks-old *ob/ob* mice was associated with the rise of *MAPK10 (Jnk3)*, *Ccnd1* and *Ccnd2* (**Fig. 5b and 5c**). Beta-cell replication in *ob/ob* mice was associated with induction of genes involved in the adaptive unfolded protein response (UPR) [27–29]. Quantitative PCR analysis revealed that the expression of UPR genes including *Atf4*, *Atf6*, *Dnacj3* (p58), *Edem1* and *Ero1* was unchanged in islet cells from 10 days old rats in which the expression of *Map3K12 (Dlk)* was silenced (**Fig. S13**). This result suggests that *Map3K12 (Dlk)* overexpression is not involved in the activation of adaptive UPR during weight gain.

We next analyzed human islet cells from non-diabetic donors with severe obesity (**Table S2**) and found also higher *MAP3K12 (DLK), MAPK10 (JNK3), CCND1 and CCND2* mRNA levels, when compared to normal-weight non-diabetic individuals (**Fig. 6**). Immunofluorescence pictures that were obtained from pancreatic sections of obese individuals without diabetes and patients with diabetes showed no apparent difference in the DLK localization (**Fig. S14**). This observation supports that induction of *MAP3K12 (DLK)* mainly account for the role of kinase and its pathway for the control of human beta-cell mass and thereby, glucose homeostasis during severe weight gain.

**DISCUSSION**

Postnatal pancreatic development is characterized by an increase in beta-cell mass, enabling adequate insulin supply for early life development. In rodents and possibly in humans, the rise in beta-cell mass before weaning results from an elevated proliferation rate [7, 8]. It has been previously shown that the robust proliferative capacity of beta-cells is maximal within the first 10 postnatal days [7]. Here we found that beta-cell *Map3k12* (*Dlk*) mRNA levels raise after birth, reach a peak at the 10$^{th}$ postnatal day, and then decline at the 20$^{th}$ postnatal day. Several evidences have led us to postulate that the stimulation of *Map3k12* (*Dlk*) mRNA levels accounts for the beta-cell proliferation in neonate rats. Map3k12 (Dlk) has multiple and paradoxical roles upon cell types and environmental context. A trophic role for Map3k12 (Dlk) has been previously postulated to induce hepatocytes proliferation upon partial hepatectomy [12, 30]. In addition, Map3k12 (Dlk) triggers fibroblast cell proliferation by regulating the expression of cell cycle regulatory proteins including Ccnd1 [12]. In beta cells, Map3k12 (Dlk) may trigger opposite effect according to its subcellular localization [19]. In contrary to the cytosolic presence of Map3k12 (Dlk), the nuclear expression of the kinase is pro-apoptotic [19]. Herein, we show that Map3k12 (Dlk) is mainly localized in the cytosol of neonate and adult rat islet cells. This observation suggests that the subcellular localization of the kinase is not modified during the postnatal development and that its overexpression is required for beta-cell proliferation to regulate the level of the key cyclins involved in postnatal beta-cell proliferation. Several lines of evidence support this hypothesis. Silencing of *Map3k12* (*Dlk*) in isolated islets from newborn rats (10 days old postnatal) dramatically reduced beta-cell proliferation in a mechanism involving the reduction of *Ccnd1* and *Ccnd2*. Importantly, the reduction of *Map3k12* (*Dlk*) level in isolated islets of 10 days old rats did not change basal beta-cell apoptosis This indicates that the observed reduction in proliferation is not the consequence of increased beta-cell death, which is in line with previous results showing that basal apoptosis of newborn and adult rat islet cells is similar [7]. In addition, *Map3k12* (*Dlk*) silencing did not enhance glucose-induced insulin secretion, nor the expression of key genes of beta-cell identity, pointing to the peculiar role of Dlk in the control of beta-cell replication during postnatal development.

We also provide some clues supporting a role for Mapk10 (Jnk3) in the mechanism whereby Map3k12 mediates the trophic effects on newborn beta-cells (**Fig. 7**). First, Map3k12 (Dlk) has been primarily identified as an upstream STK component of the signalling cascade leading to the activation Mapk/Jnk pathway including Mapk10 (Jnk3) [21]. In line with this, using a whole STKs activity assessment in islets of neonate rats, we showed that the rise of *Map3k12 (Dlk)* is associated with increased activity of several Mapk, including Mapk10 (Jnk3) and the two pro-apoptotic Mapk8 (Jnk1) and Mapk9 (Jnk2) isoforms. In beta cells, it has been postulated that in physiological conditions, Mapk10 (Jnk3) activity, may inhibit the pro-apoptotic activities of Mapk8 (Jnk1) and Mapk9 (Jnk2) [21]. Our data showing that neither apoptosis, nor Jnk1/Jnk2 activation is modified between neonate and adult islet cells support this hypothesis. In addition, we found that *Mapk10 (Jnk3)* silencing leads to decreased beta-cell proliferation. Taken together, our observations support the hypothesis that the increased Mapk10 (Jnk3) activity results from the rise in *Map3k12 (Dlk)* expression. This provides the first proof of concept supporting a physiological role for Mapk10 (Jnk3) in the control of beta-cell proliferation.

Beta-cell proliferation also contributes to the adaptation of the functional beta-cell mass under conditions characterized by a diminished insulin sensitivity such as obesity and pregnancy. In this respect, we postulated that Map3k12 (Dlk) signaling may play a pivotal role also in the mechanisms triggered to compensate for insulin resistance in adults. First, we found that the beta-cell number is reduced in Map3k12 KO mice. Second, increased *Map3k12* (*Dlk*)

mRNA was accompanied by elevated expressions of *Mapk10* (*Jnk3*), *Ccnd1* and *Ccnd2* in rodent models of obesity and pregnancy displaying an elevated beta-cell proliferation rate. As the stoichiometry of the MAPKs components is important to activate the signalling cascade [31], it is possible that induction of *Mapk10* (*Jnk3*) in compensatory islets to weight gain is the consequence of the elevated expression of Map3k12 (Dlk). In human, enhanced obesity-driven beta-cell proliferation was monitored in non-diabetic, but not in diabetic donors [5]. This result led to the hypothesis that the lack of proliferation may be causally linked to the reduced beta-cell mass and to diabetes pathogenesis. Our study showing that the *MAP3K12* (*DLK*), *MAPK10* (*JNK3*), *CCND1* and *CCND2* mRNA levels are upregulated in the islets from non-diabetic obese individuals compared to lean or diabetic obese donors, is consistent with MAP3K12 (DLK) signalling being one of the mechanisms regulating human beta-cell proliferation in severe weight gain conditions.

In conclusion, our study demonstrates that the signalling pathway activated by Map3k12 (Dlk) is a key driver of beta-cell mass expansion during critical life times were the insulin demand is increased such as postnatal development before weaning, pregnancy and obesity in both rodents and human. Abnormalities in this signalling may lead to inadequate functional beta-cell mass and eventually to diabetes development.

**Acknowledgements**

We would like to thank Mrs Laure Rolland for the technical assistance and, Antonino Bongiovanni and Meryem Tardivel from the BICeL-Campus HU Facility for access to systems and technical advice.

**Funding:**

This work was supported by grants from “Société Francophone du Diabète (SFD)”, “European Genomic Institute for Diabetes” (E.G.I.D., ANR-10-LABEX-46) and European Commission, European Research Council (GEPIDIAB 294785 to P.F.), and by a grant from the Swiss National Science Foundation (310030-169480 to RR). Human islets were provided by the European Consortium for Islet Transplantation, funded by the Juvenile Diabetes Research Foundation International".

**Duality of interests**

The authors declare that there is no duality of interest associated with the manuscript

**Contribution Statement**

MT, JKC, FP, RR, AB, PF and AA contributed to the study design and interpretation of the data. MT, SD, AB, PF and AA wrote and edited the manuscript. MT, VPL, VP, CSP, HE, RB, VG, CJ, JB, NB, GP performed the experiments and analysed the data. All authors read and approved the submission of the manuscript.

**FIGURE LEGENDS**

**Figure 1: Postnatal islet induction and beta-cell nuclear localization of Map3k12 (Dlk) in neonate rats. a)** The expression of the *Map3k12 (Dlk)* was measured by **a**) RT-qPCR and **b**) Western blotting in isolated islet of newborn rats between p1, p6, p10 and p20 postnatal days and young adult rats (p32). The mRNA levels of *Map3k12 (Dlk)* were normalized to those of Tata box binding protein *(Tbp*) and were expressed as % changes. The expression of *Map3k12 (Dlk)* at p1 was set to 100%. Data are the mean ± SEM of 3 independent experiments performed in triplicate (**, P<0.01). **b**) Western blotting was performed using total proteins (20 µg/lane) isolated from islets of 10 and 32 old days rats using an anti-Dlk (1/1000; Genetex) and anti-αTubulin (1/5000; Sigma) antibodies. The intensities of the bands were quantified using ImageJ, taking care to avoid saturation and subtracting the background. Values were expressed as the integrals (area * mean density) of each band (normalized to αTubulin band). Values from p32 were set to 100%. (**c**-**h**) Representative immunofluorescence images for Map3k12 (Dlk), insulin and glucagon in pancreatic islets of 10-days-old rat (40x magnification) using anti-Dlk (1/1000; Genetex), anti-insulin (1/100, Dako) and anti-glucagon (1/100, Sigma) antibodies. The scale bars in each picture row correspond to 20 µm. **c**), Map3k12 (Dlk) (green; **d** and **g**), and insulin (red; **f and h**) performed on fixed pancreas of newborn rats of 10 days old. Merged images were achieved to show the potential co-localization of Map3k12 (Dlk) with glucagon (**e**) or insulin (**h**). Yellow indicates the co-localization. Blue, DAPI. **i**) Detection of Map3k12 (Dlk) protein in islets nuclear-enriched fraction of 10 days old rats. Nuclear and cytosol (Cyto) proteins (20 µg/lane) were loaded onto 10% SDS-PAGE and then detected by Western blotting using an anti-Dlk (1/1000; Genetex), anti-Lamin a/c (1/1000; Abcam) and anti-Calreticulin (1/1000; Abcam) antibodies.

**Figure 2**: **Effect of Map3k12 (Dlk) silencing in beta-cell proliferation, basal beta-cell death, *Ccnd1* and *Ccnd2* mRNA levels.** The expression of the Map3k12 (Dlk) was measured in dispersed islet cells from 10 days old rats by **a**) Western Blotting experiments in dispersed islet cells of newborn rats of 10 days old, which were transfected with control siRNA (siCtl; siRNA directed against GFP) or siRNAs against Map3k12 (Dlk) (siDlk) for 48 h. beta cell proliferation was quantified by determining the percentage of insulin+ (ins+) and **b**) Ki67+ cells (n=4) or **c**) BrdU+ (n=3). **d**) Effect of siDLK on the expression of *Ccnd1* and *Ccnd2* in the islet cells of 10 days old rats. The mRNA levels were normalized to those of *Tbp* and were expressed as % changes. The data are presented as means ± SEM of 5 independent experiments performed in triplicate as determined by ANOVA (*$p < 0.05$, ***$p < 0.001$). **e**) Beta-cell death was assessed by scoring the percentage of insulin positive cells labelled with TUNEL (n=3). **f**) insulin secretion after 45 min exposure to 2 or 20 mM glucose (n= 4).

**Figure 3**: **Mapk10/Jnk3 activation by Map3k12 (Dlk) in neonate islet beta cells.** Western Blotting analysis of **a**) total and phosphorylated Mapks/Jnks (Jnk1/Jnk2 and Jnk3) and **c**) total and phosphorylated Jnk1 and Jnk2 in islets of 10 (p10) and 32 (p32) days old rats. Western blotting was achieved loading total proteins from islets of neonate (p10) and adult rats (p32) using either anti-total Jnk1/Jnk2 and p-Jnk1/Jnk2 (phospho Thr183/Tyr185; 1/1000; Thermofisher), or anti-total Jnk1/Jnk2/Jnk3 and p-Jnk1/Jnk2/Jnk3 (phospho Thr183+Thr183+Thr221,

Abcam, dilution 1:1000), or anti-αTubulin (1/5000; Sigma). **b-d**) The intensities of bands were measured using ImageJ, taking care to avoid saturation and after subtracting the background. Values are expressed as the integrals (area * mean density) of each band corresponding to p-Jnk1/2/3 or p-Jnk1/2 (p55 and p46), normalized to total Jnk1/2/3 or Jnk1/2. Values from p32 were set to 100%. **d**) The expression of *Mapk10/Jnk3* was measured by RT-qPCR in the islets of rats of p10 and p32. The results were normalized against *Tbp* and the expression levels from p10 were set to 100%. Data are the mean ± SEM of 3 independent experiments performed in triplicate (NS, P>0.05). **e**) Co-immunoprecipitation of Map3k12 (Dlk) and Mapk10 (Jnk3) in INS-1E cells. Dlk and Jnk3 proteins are pulled down by the anti-Dlk (1/1000; Eurogentec) or anti-Jnk3 antibodies (1/1000, Cell Signaling) but not with control anti-Hdac1 antibody (1/1000; Santa Cruz). Phosphorylation level of Jnk3 (Thr183/Tyr185 residue) after Jnk3 immunoprecipitation in response to **f**) Map3k12 (Dlk) silencing (siDlk) or **g**) Map3k12 (pcDlk) overexpression in INS-1E cells. Immunoblotting were achieved using either anti-Dlk (1/1000; Eurogentec), or anti-Jnk3 (1/1000, Cell Signaling) or anti phospho-Jnk3 (Thr183/Tyr185, 1/1000, Cell Signaling). The figures show the result of a representative experiment out of three.

**Figure 4**: **Effect of Mapk10 (Jnk3) silencing in beta-cell proliferation and *Ccnd1* and *Ccnd2* mRNA levels** **a**) Newborn rat islet cells were transfected with control siRNA (siCtl; siRNA directed against GFP) or siRNAs against Jnk3 for 48 h and *Jnk3* mRNA levels were measured by RT-qPCR. beta cell proliferation was quantified by determining the percentage of insulin+ (ins+) and **b**) Ki67+ cells (n=3) and **c**) BrdU. **d**) Effect of siJnk3 on the expression of indicated genes in the islet cells of 10 days old rats. Data are the means ± SEM of 3 independent experiments performed in triplicate (*$p < 0.05$, ***$p < 0.001$).

**Figure 5**: **Measurement of islets *Map3k12 (Dlk)*, *Ccnd1* and *Ccnd2* expression changes in mice model of pregnancy and obesity. a**) the expression of *Map3k12 (Dlk)*, *Mapk10* (*Jnk3*), *Ccnd1* and *Ccnd2*, was measured by RT-qPCR in the islets of female rats at indicated gestational days 10 (G10), 12 (G12), 14 (G14), and 3 days post-partum (P3). The results are expressed as % of the level in non-pregnant rats (Ctl). **b**) Measurement of *Map3k12 (Dlk) and Mapk10* (*Jnk3*) and **c**) *Ccnd1 and Ccnd2* in islets isolated from *ob/ob* mice at the indicated ages and of age-matched controls. The data represent the mean ± SEM of 4 animals per group.

**Figure 6: *MAP3K12 (DLK)* in isolated human islet cells from lean and obese donors.** The mRNA levels of *MAP3K12 (DLK) MAPK10 (JNK3), CCND1* and *CCND2* were measured in isolated human islets from lean donors (N=7), obese individuals without diabetes donors (N=7) and obese patients with diabetes (N=5). The data were normalized against the *RPLP27* and were expressed as the fold changes over the lean controls. Data are the mean of ± SEM (***, P<0.001; **, P<0.01; by ANOVA analysis).

**Figure 7: Schematic representation of beta cell mass regulation by Map3k12 (Dlk).**

**REFERENCES**


1. Chen C, Cohrs CM, Stertmann J, et al (2017) Human beta cell mass and function in diabetes: Recent advances in knowledge and technologies to understand disease pathogenesis. Mol Metab 6:943–957. https://doi.org/10.1016/j.molmet.2017.06.019
2. Golson ML, Misfeldt AA, Kopsombut UG, et al (2010) High Fat Diet Regulation of β-Cell Proliferation and β-Cell Mass. Open Endocrinol J 4:. https://doi.org/10.2174/1874216501004010066
3. Baeyens L, Hindi S, Sorenson RL, German MS (2016) β-Cell Adaptation in Pregnancy. Diabetes Obes Metab 18:63–70. https://doi.org/10.1111/dom.12716
4. Davis DB, Lavine JA, Suhonen JI, et al (2010) FoxM1 Is Up-Regulated by Obesity and Stimulates β-Cell Proliferation. Mol Endocrinol 24:1822–1834. https://doi.org/10.1210/me.2010-0082
5. Hanley SC, Austin E, Assouline-Thomas B, et al (2010) β-Cell Mass Dynamics and Islet Cell Plasticity in Human Type 2 Diabetes. Endocrinology 151:1462–1472. https://doi.org/10.1210/en.2009-1277
6. Mezza T, Kulkarni RN (2014) The regulation of pre- and post-maturational plasticity of mammalian islet cell mass. Diabetologia 57:1291–1303. https://doi.org/10.1007/s00125-014-3251-7
7. Jacovetti C, Matkovich SJ, Rodriguez-Trejo A, et al (2015) Postnatal β-cell maturation is associated with islet-specific microRNA changes induced by nutrient shifts at weaning. Nat Commun 6:. https://doi.org/10.1038/ncomms9084
8. Meier JJ, Butler AE, Saisho Y, et al (2008) Beta-cell replication is the primary mechanism subserving the postnatal expansion of beta-cell mass in humans. Diabetes 57:1584–1594. https://doi.org/10.2337/db07-1369
9. Gregg BE, Moore PC, Demozay D, et al (2012) Formation of a Human β-Cell Population within Pancreatic Islets Is Set Early in Life. J Clin Endocrinol Metab 97:3197–3206. https://doi.org/10.1210/jc.2012-1206
10. Kushner JA, Ciemerych MA, Sicinska E, et al (2005) Cyclins D2 and D1 Are Essential for Postnatal Pancreatic β-Cell Growth. Mol Cell Biol 25:3752–3762. https://doi.org/10.1128/MCB.25.9.3752-3762.2005
11. Bononi A, Agnoletto C, De Marchi E, et al (2011) Protein Kinases and Phosphatases in the Control of Cell Fate. In: Enzyme Res. 329098. doi: 10.4061/2011/329098
12. Daviau A, Couture J-P, Blouin R (2011) Loss of DLK expression in WI-38 human diploid fibroblasts induces a senescent-like proliferation arrest. Biochem Biophys Res Commun 413:282–287. https://doi.org/10.1016/j.bbrc.2011.08.086
13. Kulkarni RN, Mizrachi E-B, Ocana AG, Stewart AF (2012) Human β-Cell Proliferation and Intracellular Signaling: Driving in the Dark Without a Road Map. Diabetes 61:2205–2213. https://doi.org/10.2337/db12-0018
14. Baggio LL, Drucker DJ (2007) Biology of incretins: GLP-1 and GIP. Gastroenterology 132:2131–2157. https://doi.org/10.1053/j.gastro.2007.03.054
15. Vantyghem MC, Kerr-Conte J, Arnalsteen L, et al (2009) Primary graft function, metabolic control, and graft survival after islet transplantation. Diabetes Care 32:1473–1478. https://doi.org/10.2337/dc08-1685
16. Hirai S, Cui DF, Miyata T, et al (2006) The c-Jun N-Terminal Kinase Activator Dual Leucine Zipper Kinase Regulates Axon Growth and Neuronal Migration in the Developing Cerebral Cortex. J Neurosci 26:11992–12002. https://doi.org/10.1523/JNEUROSCI.2272-06.2006
17. Brajkovic S, Ferdaoussi M, Pawlowski V, et al (2016) Islet Brain 1 Protects Insulin Producing Cells against Lipotoxicity. J Diabetes Res 2016:. https://doi.org/10.1155/2016/9158562
18. Abderrahmani A, Yengo L, Caiazzo R, et al (2018) Increased Hepatic PDGF-AA Signaling Mediates Liver Insulin Resistance in Obesity-Associated Type 2 Diabetes. Diabetes 67:1310–1321. https://doi.org/10.2337/db17-1539
19. Wallbach M, Duque Escobar J, Babaeikelishomi R, et al (2016) Distinct functions of the dual leucine zipper kinase depending on its subcellular localization. Cell Signal 28:272–283. https://doi.org/10.1016/j.cellsig.2016.01.002
20. Holzman LB, Merritt SE, Fan G (1994) Identification, molecular cloning, and characterization of dual leucine zipper bearing kinase. A novel serine/threonine protein kinase that defines a second subfamily of mixed lineage kinases. J Biol Chem 269:30808–30817
21. Beeler N, Riederer BM, Waeber G, Abderrahmani A (2009) Role of the JNK-interacting protein 1/islet brain 1 in cell degeneration in Alzheimer disease and diabetes. Brain Res Bull 80:274–281. https://doi.org/10.1016/j.brainresbull.2009.07.006
22. Stahnke M-J, Dickel C, Schröder S, et al (2014) Inhibition of human insulin gene transcription and MafA transcriptional activity by the dual leucine zipper kinase. Cell Signal 26:1792–1799. https://doi.org/10.1016/j.cellsig.2014.04.006
23. Jacovetti C, Abderrahmani A, Parnaud G, et al (2012) MicroRNAs contribute to compensatory β cell expansion during pregnancy and obesity. J Clin Invest 122:3541–3551. https://doi.org/10.1172/JCI64151

24. Rieck S, Kaestner KH (2010) Expansion of beta-cell mass in response to pregnancy. Trends Endocrinol Metab 21:151–158. https://doi.org/10.1016/j.tem.2009.11.001
25. Mosser RE, Maulis MF, Moullé VS, et al (2015) High-fat diet-induced β-cell proliferation occurs prior to insulin resistance in C57Bl/6J male mice. Am J Physiol - Endocrinol Metab 308:E573–E582. https://doi.org/10.1152/ajpendo.00460.2014
26. Lindström P (2010) beta-cell function in obese-hyperglycemic mice [ob/ob Mice]. Adv Exp Med Biol 654:463–477. https://doi.org/10.1007/978-90-481-3271-3_20
27. Plaisance V, Brajkovic S, Tenenbaum M, et al (2016) Endoplasmic Reticulum Stress Links Oxidative Stress to Impaired Pancreatic Beta-Cell Function Caused by Human Oxidized LDL. PLoS ONE 11:. https://doi.org/10.1371/journal.pone.0163046
28. Chan JY, Luzuriaga J, Bensellam M, et al (2013) Failure of the adaptive unfolded protein response in islets of obese mice is linked with abnormalities in β-cell gene expression and progression to diabetes. Diabetes 62:1557–1568. https://doi.org/10.2337/db12-0701
29. Cnop M, Toivonen S, Igoillo-Esteve M, Salpea P Endoplasmic reticulum stress and eIF2α phosphorylation: the Achilles heel of pancreatic β cells. Mol Metab. https://doi.org/10.1016/j.molmet.2017.06.001
30. Douziech M, Grondin G, Loranger A, et al (1998) Zonal Induction of Mixed Lineage Kinase ZPK/DLK/MUK Gene Expression in Regenerating Mouse Liver. Biochem Biophys Res Commun 249:927–932. https://doi.org/10.1006/bbrc.1998.9249
31. Kragelj J, Palencia A, Nanao MH, et al (2015) Structure and dynamics of the MKK7-JNK signaling complex. Proc Natl Acad Sci U S A. 112(11):3409-3414. doi: 10.1073/pnas.1419528112

**Fig. 1**

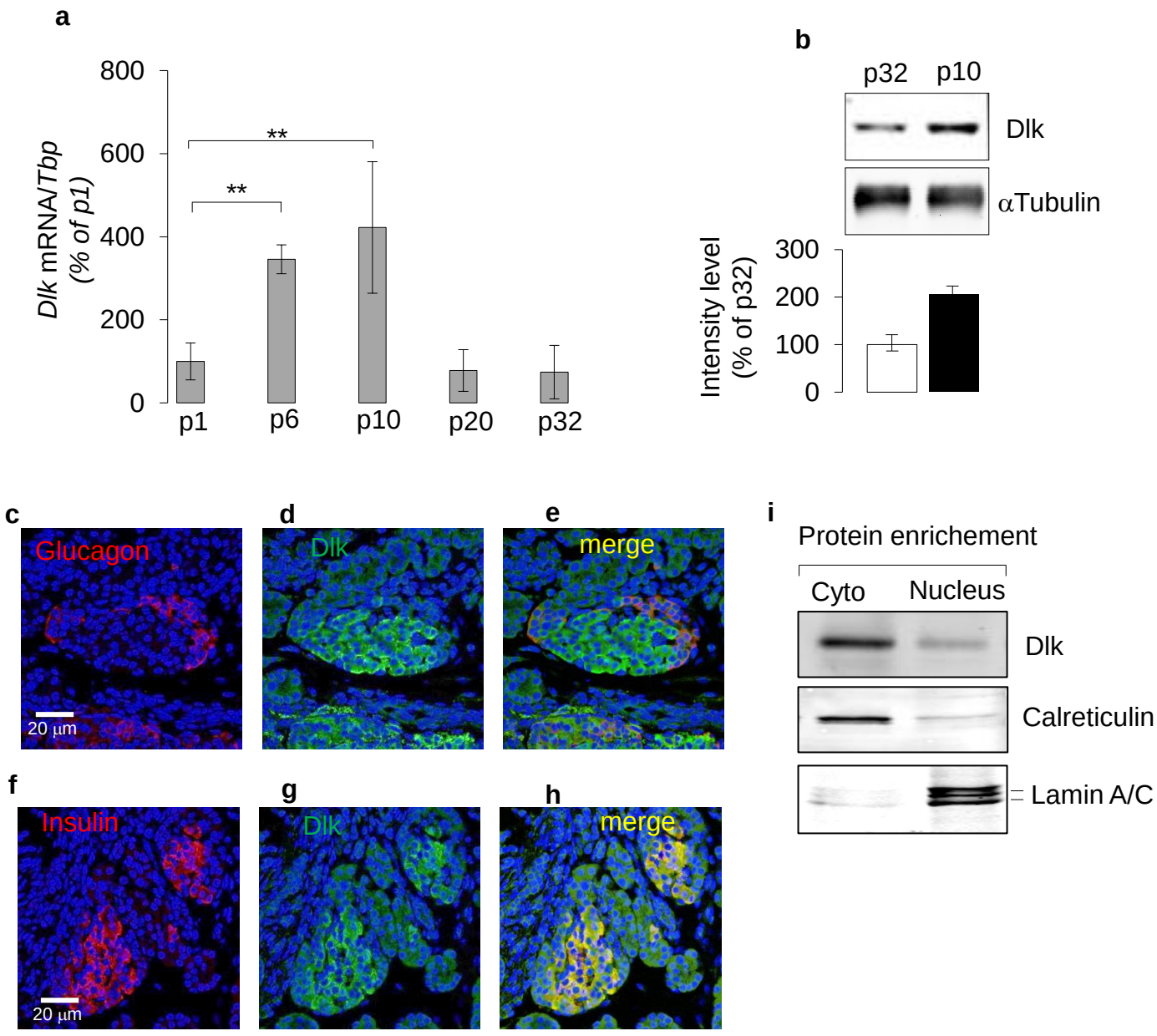
a
800
600
400
200
0
Dlk mRNA/Tbp
(% of p1)
**
**
p1
p6
p10
p20
p32
b
p32
p10
Dlk
αTubulin
300
200
100
0
Intensity level
(% of p32)
c
Glucagon
20 μm
d
Dlk
e
merge
f
Insulin
20 μm
g
Dlk
h
merge
i
Protein enrichement
Cyto
Nucleus
Dlk
Calreticulin
Lamin A/C

**Fig. 2**

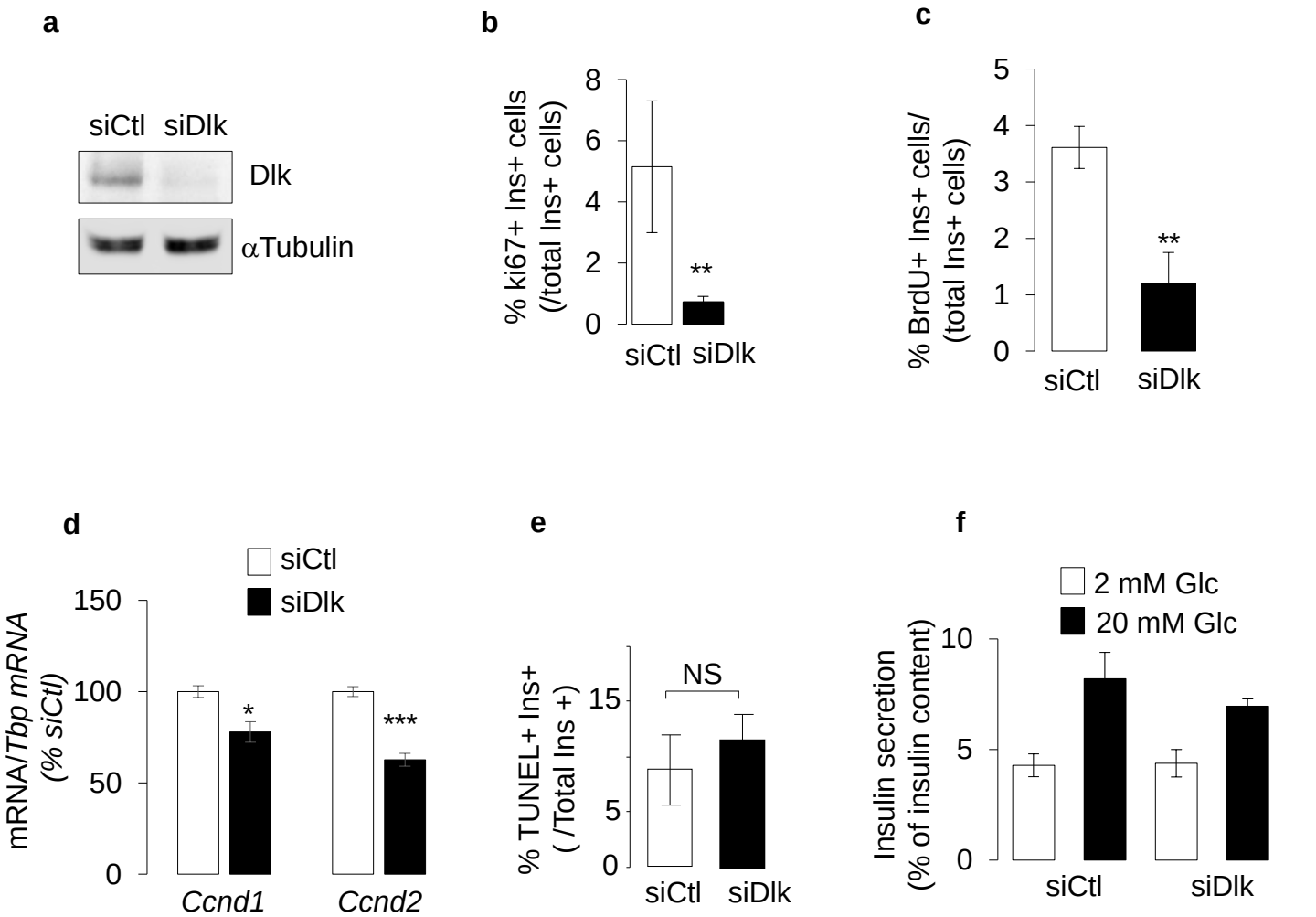
a
siCtl siDlk
Dlk
αTubulin
b
% ki67+ Ins+ cells (/total Ins+ cells)
8
6
4
2
0
**
siCtl siDlk
c
% BrdU+ Ins+ cells/ (total Ins+ cells)
5
4
3
2
1
0
**
siCtl siDlk
d
siCtl
siDlk
mRNA/Tbp mRNA (% siCtl)
150
100
50
0
*
***
Ccnd1
Ccnd2
e
% TUNEL+ Ins+ ( /Total Ins +)
NS
15
5
0
siCtl siDlk
f
2 mM Glc
20 mM Glc
Insulin secretion (% of insulin content)
10
5
0
siCtl
siDlk

**Fig. 3**

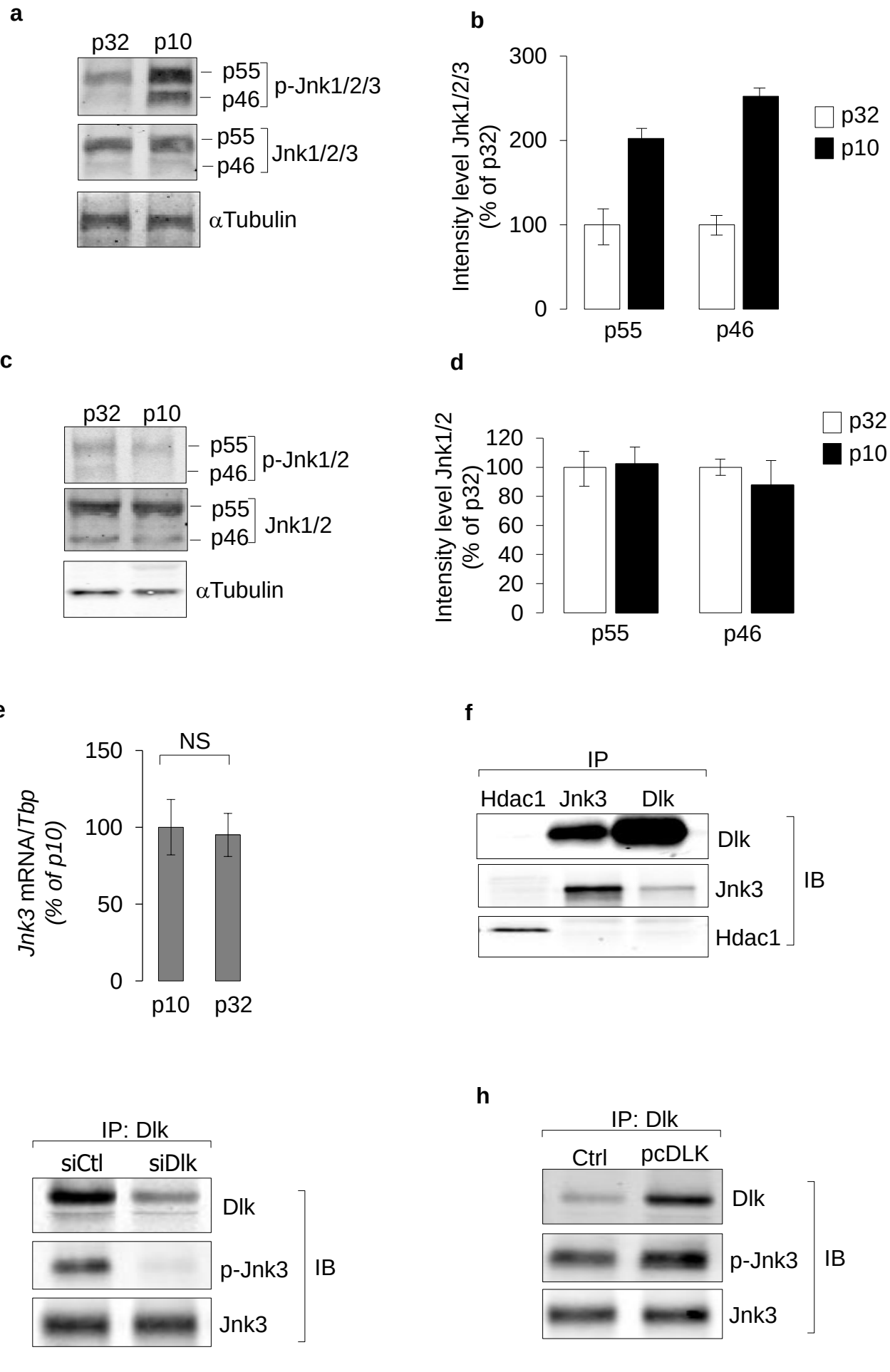
a
p32
p10
p55
p46
p-Jnk1/2/3
p55
p46
Jnk1/2/3
αTubulin
b
Intensity level Jnk1/2/3 (% of p32)
300
200
100
0
p32
p10
p55
p46
c
p32
p10
p55
p46
p-Jnk1/2
p55
p46
Jnk1/2
αTubulin
d
Intensity level Jnk1/2 (% of p32)
120
100
80
60
40
20
0
p32
p10
p55
p46
e
NS
Jnk3 mRNA/Tbp (% of p10)
150
100
50
0
p10
p32
f
IP
Hdac1
Jnk3
Dlk
Dlk
Jnk3
Hdac1
IB
g
IP: Dlk
siCtl
siDlk
Dlk
p-Jnk3
Jnk3
IB
h
IP: Dlk
Ctrl
pcDLK
Dlk
p-Jnk3
Jnk3
IB

**Fig 4**

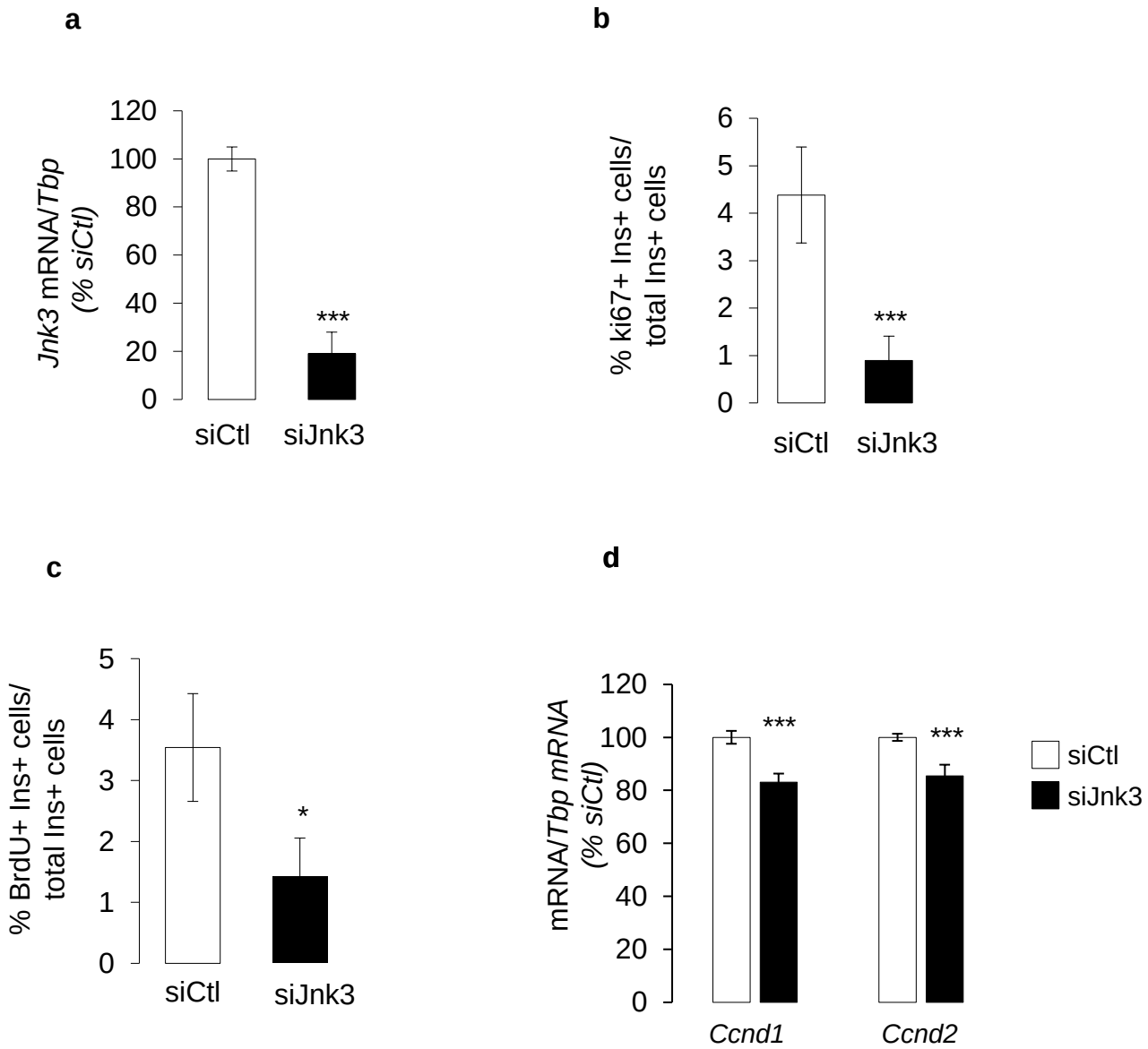
a
Jnk3 mRNA/Tbp (% siCtl)
120
100
80
60
40
20
0
***
siCtl
siJnk3
b
% ki67+ Ins+ cells/ total Ins+ cells
6
5
4
3
2
1
0
***
siCtl
siJnk3
c
% BrdU+ Ins+ cells/ total Ins+ cells
5
4
3
2
1
0
*
siCtl
siJnk3
d
mRNA/Tbp mRNA (% siCtl)
120
100
80
60
40
20
0
***
***
Ccnd1
Ccnd2
siCtl
siJnk3

**Fig. 5**

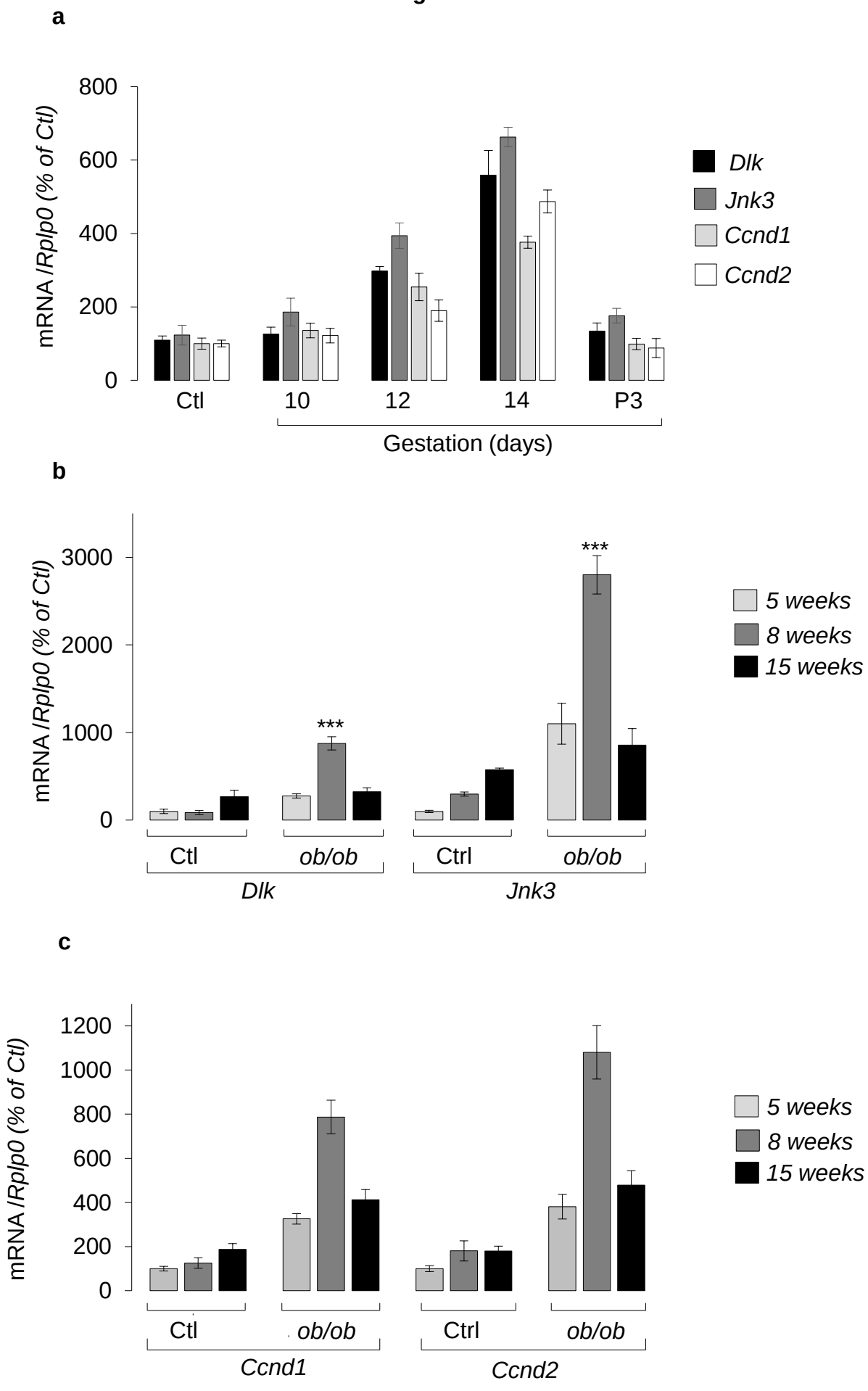
a
800
600
400
200
0
mRNA /Rplp0 (% of Ctl)
Ctl
10
12
14
P3
Gestation (days)
Dlk
Jnk3
Ccnd1
Ccnd2
b
3000
2000
1000
0
mRNA /Rplp0 (% of Ctl)
***
***
Ctl
ob/ob
Ctrl
ob/ob
Dlk
Jnk3
5 weeks
8 weeks
15 weeks
c
1200
1000
800
600
400
200
0
mRNA /Rplp0 (% of Ctl)
Ctl
ob/ob
Ctrl
ob/ob
Ccnd1
Ccnd2
5 weeks
8 weeks
15 weeks

**Fig. 6**

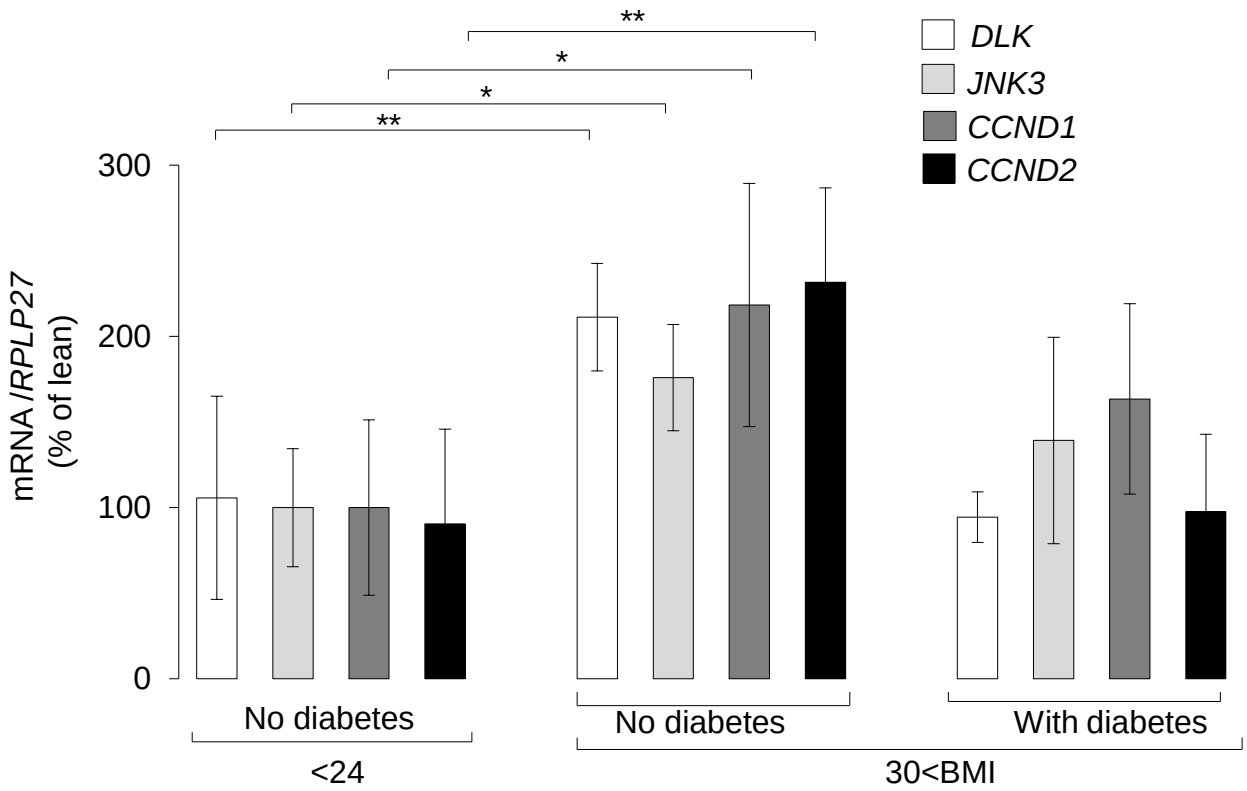
**
*
*
**
DLK
JNK3
CCND1
CCND2
300
200
100
0
mRNA /RPLP27
(% of lean)
No diabetes
No diabetes
With diabetes
<24
30<BMI

**Fig. 7**

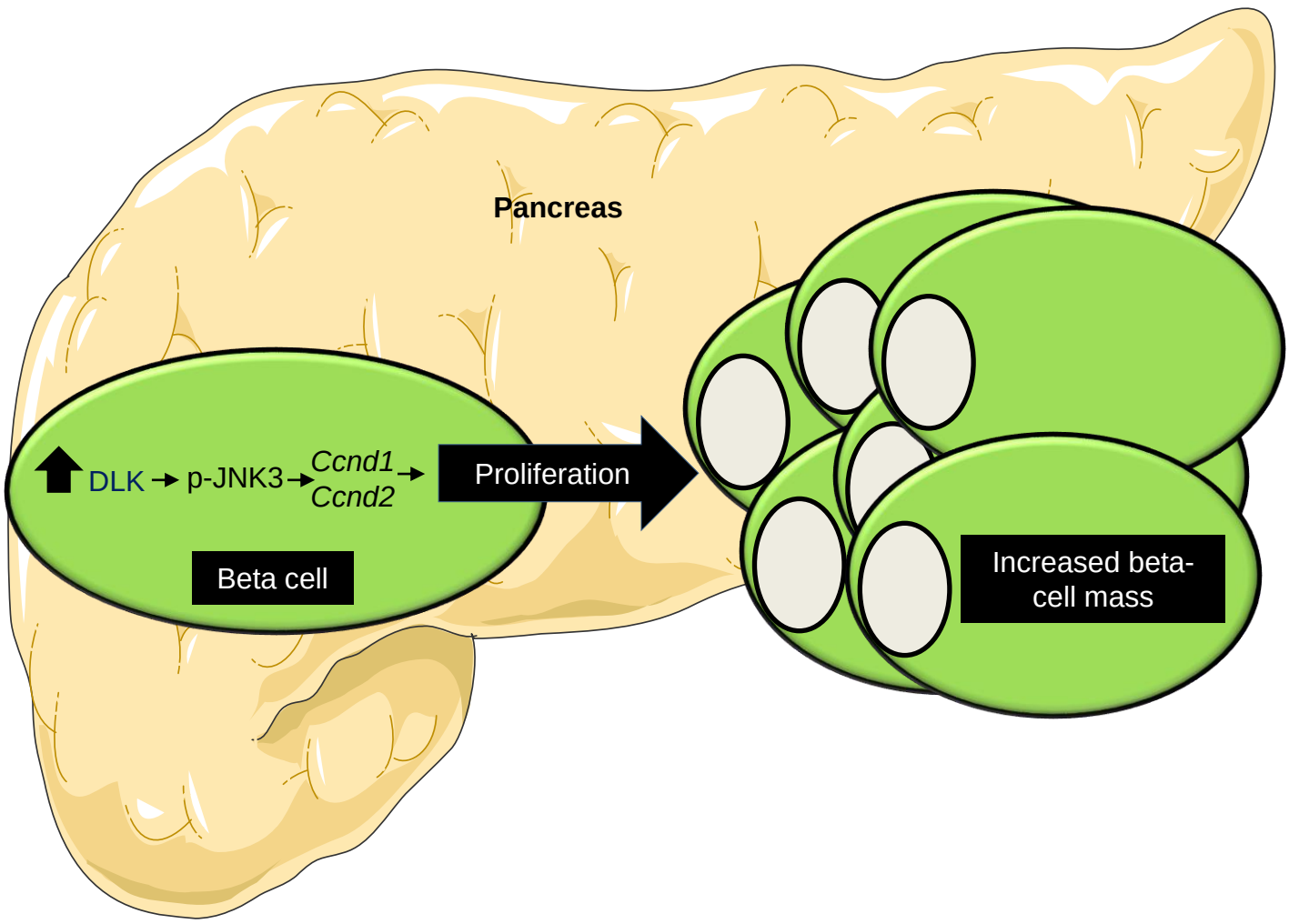
Pancreas
DLK
p-JNK3
Ccnd1
Ccnd2
Proliferation
Beta cell
Increased beta-cell mass

**Supplemental Information**

**Table S1:** List of antibodies

| Antibodies | Suppliers | Catalogs reference | Dilution/buffer |
|---|---|---|---|
| DLK (for IF, IP, and Western Blotting) | Genetex | GTX124127 | 1/1000 in TBST 5% BSA |
| Insulin | DAKO | A0564 | 1/100 in PBS |
| Glucagon | Sigma-Aldrich | G2654 | 1/100 in PBS |
| Ki67 | Abcam | Ab15580 | 1/700 in PBS/Saponin/1%BSA |
| BrdU | BD biosciences | 347580 | 1/500 in PBS/Saponin/1%BSA |
| Alexa Fluor 488nm Goat anti mouse IgG (H+L) | ThermoFischer | R37120 | 1/500 in water/1%BSA |
| Alexa Fluor 594nm Goat anti mouse IgG (H+L) | ThermoFischer | R37121 | 1/500 in water/1%BSA |
| Alexa Fluor 488nm Goat anti guinea-pig IgG (H+L) | ThermoFischer | A11073 | 1/500 in water/1%BSA |
| Alexa Fluor 594nm Goat anti guinea-pig IgG (H+L) | ThermoFischer | A11076 | 1/500 in water/1%BSA |
| α-Tubulin | Sigma-Aldrich | T5168 | 1/5000 in TBST/5% milk |
| JNK1/JNK2/JNK3 | Cell Signaling | #9252 | 1/1000 in TBST/5% BSA |
| p-JNK1/2 (T183 + Y185) | Abcam | Ab4831 | 1/1000 in TBST/5% BSA |
| p-JNK1/2/3 (T183 + T221) | Abcam | Cell Signaling | #4671 |
| JNK1/2 | ThermoFischer | AHO1362 | 1/1000 in TBST/5% BSA |
| JNK3 | Cell Signaling | #2305 | 1/1000 in TBST/5% BSA |
| Anti-rabbit IRDye 800 | Rockland Immunochemicals | 611-745-127 | 1/5000 in TBST/5% milk |
| Anti-mouse IRDye 700 | Rockland Immunochemicals | 18-4417-32 | 1/5000 in TBST/5% milk |

**Table S2**: Characteristics of human donors

| | Donors | Gender (H/F) | Age (Years) | BMI ($Kg/m^2$) | Hba1c % (mmol/mol) | Purity (%) | Viability (%) |
|---|---|---|---|---|---|---|---|
| **Lean** | D1 | F | 57 | 23.9 | 5.4 | 90 | 94.3 |
| | D2 | F | 50 | 22.6 | 4.8 | 50 | 89.1 |
| | D3 | M | 58 | 24.7 | 5.2 | 55 | 98.7 |
| | D4 | M | 58 | 24.9 | 5.3 | 50 | 95 |
| | D5 | F | 62 | 26.2 | 4.2 | 90 | 94.2 |
| | D6 | M | 55 | 23.5 | 5.0 | 90 | 96.9 |
| | D7 | F | 49 | 18.8 | 5.0 | 70 | 95.9 |
| **Obese** | D8 | M | 66 | 36.9 | 5.3 | 80 | 99 |
| | D9 | F | 47 | 31.1 | 5.6 | 85 | 96 |
| | D10 | F | 51 | 34.4 | 5.6 | 80 | 97.3 |
| | D11 | F | 57 | 33.2 | 5.6 | 80 | 95 |
| | D12 | M | 47 | 33.8 | 5.2 | 70 | 95.6 |
| | D13 | F | 49 | 31.2 | 5.3 | 50 | 97.1 |

| | | | | | | | |
|---|---|---|---|---|---|---|---|
| | D14 | M | 51 | 30.7 | 5.2 | 90 | 95.7 |
| **Obese with diabetes** | D15 | M | 58 | 32.9 | 7.2 | 80 | 87.6 |
| | D16 | M | 62 | 32.7 | 7.5 | 90 | 96.3 |
| | D17 | M | 58 | 33.8 | 6.6 | 70 | 91.9 |
| | D18 | M | 45 | 32.9 | 7.4 | 70 | 96.6 |
| | D19 | F | 56 | 34.5 | 7.9 | 70 | 98.4 |

**Legends of Supplementary figures**

**Supplementary Figure 1: a)** Overexpression of Dlk in INS-1E cells was measured by Western Blotting experiments. INS-1E cells were transiently transfected in 24 wells-plate with the control plasmid (-, *open bar*) or plasmid coding for Dlk (pcDlk, *filled bar*) at different concentrations (+: 1mg; ++: 2mg and +++: 4 mg) for 48 hrs. Immunoblottings were achieved using either anti-Dlk (1/1000; Genetex) or or anti-αTubulin (1/5000; Sigma). The figure shows the result of a representative experiment out of three. **b**) The rate of apoptosis was determined by scoring cells displaying pyknotic (visualized with Hoechst 33342). The counting was performed blind by two different experimenters. Data are the means ± SEM of 3 independent experiments performed in triplicate. *,$p<0.05$

**Supplementary Figure 2:** Representative immunofluorescence images of islets from adult rats (p32). Scale bar = 20 µm. Red: insulin or glucagon, green: Dlk.

**Supplementary Figure 3:** Representative histological pictures that enabled the quantification of dissociated beta-cell proliferation upon Dlk silencing (siDlk). Scale bar = 20 µm. Blue: DAPI, red: insulin, green: **a**) ki67 or **b**) BrdU.

**Supplementary Figure 4:** Effect of siDLK on the expression of genes involved in the control of beta-cell apoptosis in the islet cells of 10 days old rats. The mRNA levels were measured by RT-qPCR and were normalized to those of *Tbp*. The expression of genes from control cells (transfected with siGFP) was set to 100% and the change was expressed as % changes. Data are the means ± SEM of 3 independent experiments performed in triplicate. NS: Not Significant

**Supplementary Figure 5:** Effect of siDLK on the expression of beta-cell identity genes including *Pdx1*, *Glut2*, *Ins2*, *GCK*, *Mafa*, *Kir6.2*, *Nkx6.1* and *Znt8* in the islet cells of 10 days old rats. The mRNA levels were measured by RT-qPCR and were normalized to those of *Tbp*. The expression of genes from control cells (siGFP) was set to 100% and the change was expressed as % changes. Data are the means ± SEM of 3 independent experiments performed in triplicate. NS: Not Significant

**Supplementary Figure 6:** Putative modulated Serine Threonine kinases activity in islet cells of 10 days old rats when compared to adult rats. The ST kinome analysis was achieved using Serine Threonine Kinases microarrays, which were purchased from PamGene International BV. Each array contained 140 target peptides as well as 4 control peptides. Sample incubation, detection, and analysis were performed in a PamStation 12 according to the manufacturer's instructions. Briefly, extracts from islets cells were made using M-PER mammalian extraction buffer (Thermo Scientific) for 20 minutes on ice. Kinase reactions were performed for 1 hour with 5 µg of total extract and 400 µM ATP at 30°C. Phosphorylated peptides were detected with an anti-rabbit–FITC antibody that recognizes a pool of anti–phospho serine/threonine antibodies. The instrument contains a 12-bit CCD camera suitable for imaging of FITC-labeled arrays. The images obtained from the phosphorylated arrays were quantified using the BioNavigator software (PamGene International BV), and the list of peptides whose phosphorylation was significantly different between control and test conditions was uploaded to GeneGo for pathway analysis. Specific and positive kinase statistic (in red) show higher activity in islets of 10 compared with adult islets.

**Supplementary Figure 7**: Beta-cell death in 10 days old (p10) and young rats (p32). Beta-cell death was assessed by scoring the percentage of insulin positive (ins+) cells labelled with TUNEL assay. NS: Not Significant

**Supplementary Figure 8**: **a**) Mapks/Jnks activation in response to Map3k12 (Dlk) silencing and **b**) Map3k12 overexpression (pcDlk) in INS-1E cells. Jnk phosphorylation and total Jnk expression were monitored from total proteins of INS-1E cells that were cultured with 10 ng/ml Interleukin 1b (IL) for the indicated times. The figure shows the results of a representative experiment out of three. Immunoblotting experiment was achieved using either anti-Dlk (1/1000; Genetex) or anti-Phospho-Jnk (Thr183/Tyr185, 1/1000, Cell Signaling) or anti-Jnk antibodies (total Jnk, 1/1000, Cell Signaling), or anti-aTubulin (1/500, Sigma).

**Supplementary Figure 9:** Interaction of Map3k12 (Dlk) with Jnk3. Association of Map3k12 and Mapk10 (Jnk3). Plasmids coding for Map3k12 (Dlk, D) and Mapk10 (Jnk3, J) were co-transfected in HeLa cells cultured in DMEM medium supplemented with 10% fetal calf serum, 50 U/ml penicillin and 50 µg/ml streptomycin for 48 hrs. Cells were harvested by trypsinization and washed with PBS, then lysed in lysis buffer containing 0.4% Triton X-100, HEPES (40 mmol/l pH 7.4), EDTA (1 mmol/l), NaCl (120 mmol/l) or Co-IP lysis buffer B (0.5% Triton X-100, 20 mM Hepes (pH 7.4), 150 mM NaCl, 1.5 mM $MgCl_2$, 2 mM EGTA), supplemented with 10 µg/ml each aprotinin and leupeptin, 1 mM PMSF. Cell lysates were cleared by centrifugation at 4°C. Equal amounts of total protein between samples were incubated with the pre-washed appropriate affinity gel overnight. Then, beads were washed four times with Co-IP lysis buffer, and bound proteins were eluted with SDS sample buffer. Samples were resolved by SDS–PAGE for immunoblot analysis (IB) of Map3k12 (Dlk) and Mapk10 (Jnk3) were achieved after Map3k12 (Dlk) or Mapk10 (Jnk3) immunoprecipitation using anti-Dlk (1/1000; Genetex) and anti-Jnk3 (1/1000, Cell Signaling). The figure shows the results of a representative experiment out of three.

**Supplementary Figure 10:** Representative histological pictures that enabled the quantification of dissociated beta-cell proliferation upon Jnk3 silencing (siJnk3). Scale bar = 20 µm. Blue: DAPI, red: insulin, green: **a**) ki67 or **b**) BrdU.

**Supplementary Figure 11:** Expression of insulin and beta-cell mass in Map3k12 (Dlk) knock out mice embryos. **a)** Representative images of immunofluorescence staining for insulin (red; **a** and **d**), and glucagon (green; **b** and **e**) on fixed embryos (e18.5) of wild type or heterozygous (Ctl) and knockout mice ($Dlk^{-/-}$). Merged images (**c** and **f**) showed the localization of glucagon and insulin within the islets of Ctl and $Dlk^{-/-}$ mice. Blue, DAPI. Fluorescence intensities of insulin (**g**) and glucagon (**h**) were quantified. Quantification of insulin and glucagon. **i**) Morphometric analysis of Ctl and $Dlk^{-/-}$ mice (n = 3) insulin and glucagon positive area in e18.5 embryos. Columns represent mean ± SEM, *p < 0.05.

**Supplementary Figure 12:** Representative immunofluorescence images of islets from control mice (age-matched) and *ob/ob* mice (8 weeks old). Scale bar = 20 µm. Red: insulin, green: Dlk, blue: DAPI.

**Supplementary Figure 13:** Effect of siDLK on the expression of unfolded protein response marker genes including *Atf4*, *Atf6*, *Dnacj3*, *Edem1* and *Ero1* in islet cells from 10 days old rats. The mRNA levels were normalized to those of Tata box binding protein *(Tbp*) and were expressed as % changes over those of control cells transfected with siCtl (siGFP). The expression of *Map3k12 (Dlk)* at p1 was set to 100%. Data are the mean ± SEM of 3 independent experiments performed in triplicate. NS: Not Significant

**Supplementary Figure 14:** Representative immunofluorescence images for Map3k12 (Dlk) and insulin in pancreatic islets of **a**) non diabetic obese individual and **b**) obese patient with diabetes (40x magnification) using anti-Dlk (1/1000; Genetex), anti-insulin (1/100, Dako) antibodies. The scale bars are representative of each picture row and correspond to 20 µm.

**Fig. S1**

**a**

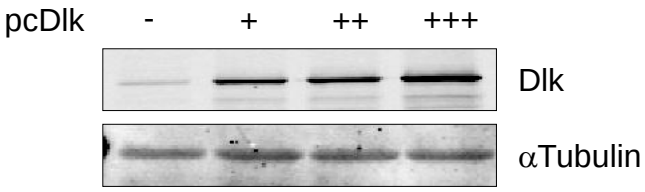


**b**

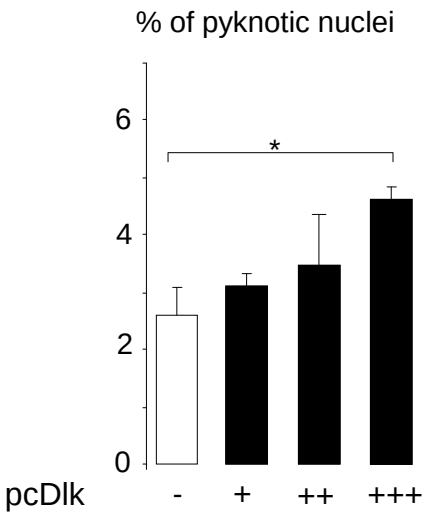

**Fig. S2**

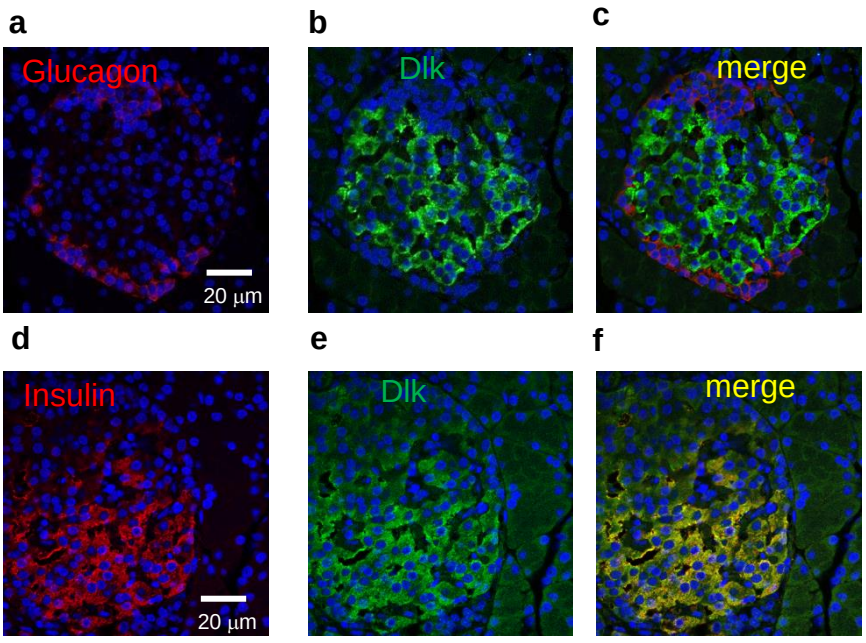

**Fig. S3**

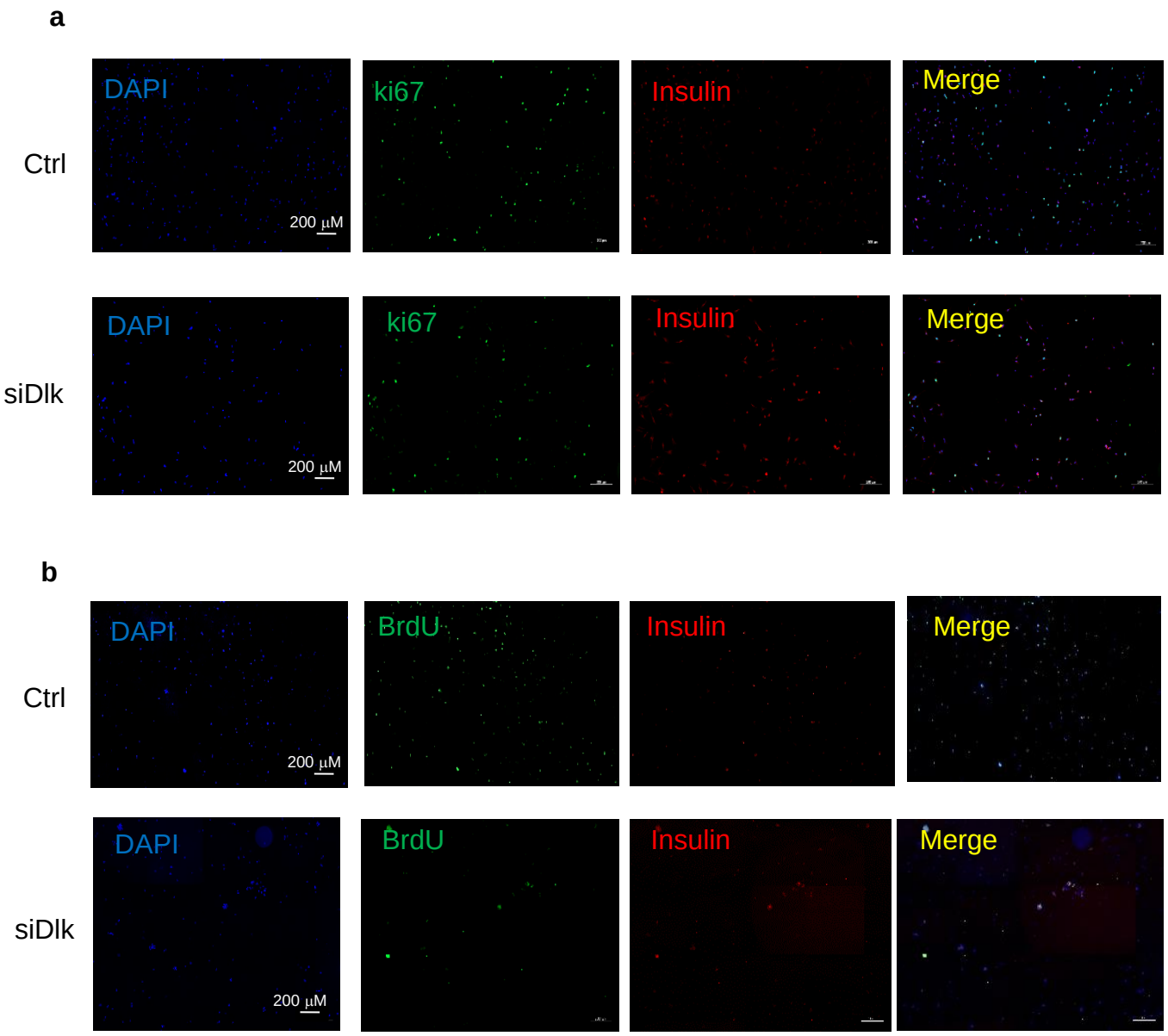
a
Ctrl
DAPI
ki67
Insulin
Merge
200 μM
siDlk
DAPI
ki67
Insulin
Merge
200 μM
b
Ctrl
DAPI
BrdU
Insulin
Merge
200 μM
siDlk
DAPI
BrdU
Insulin
Merge
200 μM

**Fig. S4**

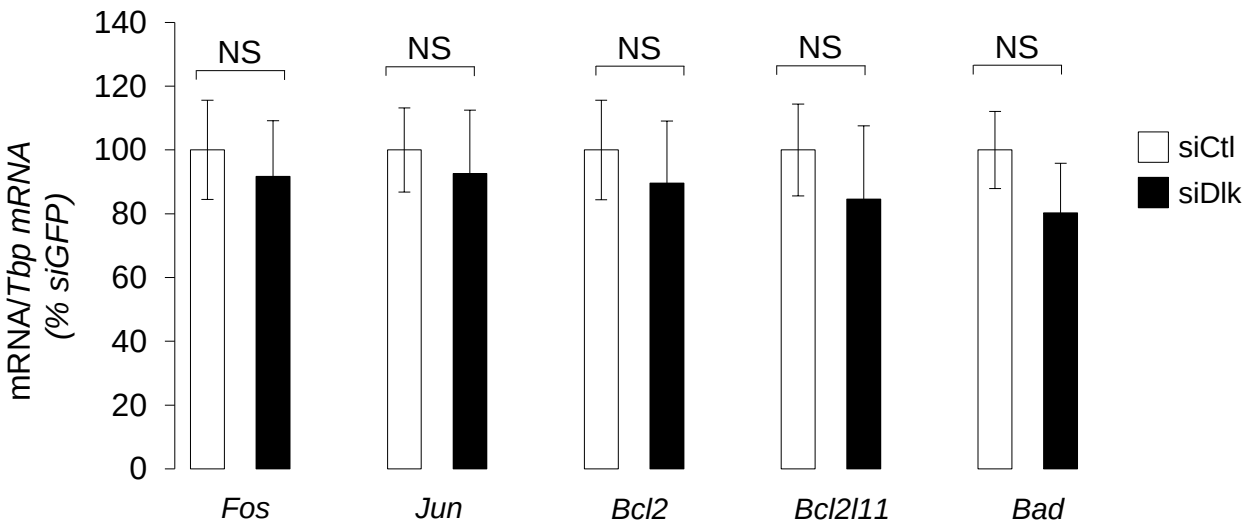
140
120
100
80
60
40
20
0
mRNA/Tbp mRNA
(% siGFP)
NS
NS
NS
NS
NS
Fos
Jun
Bcl2
Bcl2l11
Bad
siCtl
siDlk

**Fig. S5**

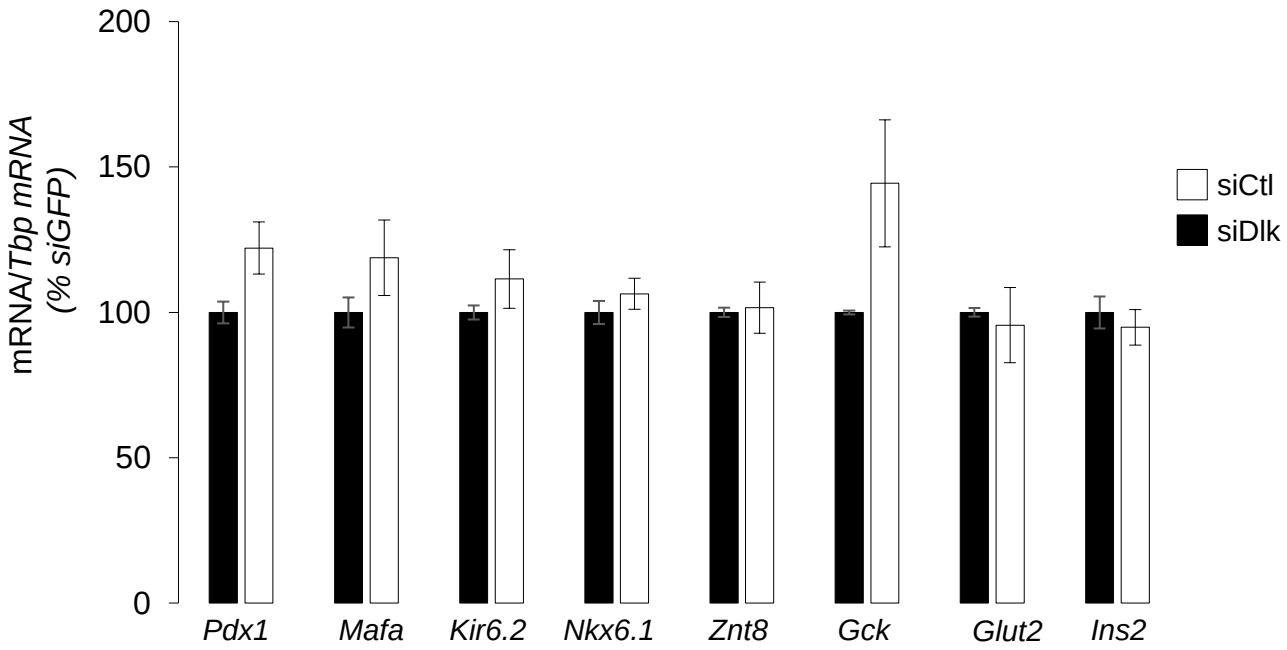
200
150
100
50
0
mRNA/Tbp mRNA
(% siGFP)
siCtl
siDlk
Pdx1
Mafa
Kir6.2
Nkx6.1
Znt8
Gck
Glut2
Ins2

# Fig. S6


Jnk3
p38g MAPK (MAPK12)
p38d MAPK (MAPK13)
p38b MAPK (MAPK11)
JNK3 (MAPK10)
JNK2 (MAPK9)
JNK1 (MAPK8)
ERK5 (MAPK7)
ERK2 (MAPK1)
ERK1
CDKL2
CDK2
CDK1 (CDC2)
p38a MAPK (MAPK14)
CDKL5 (STK9)
ADCK3 (LOC56997)
CDKL4 (AA626859)
DYRK1A
CDK3
HIPK3
HIPK2
HIPK1 (BE180036)
DYRK1B
ERK7 (BI916334)
PKCI (PRKCI)
PIM2
DCAMKL3 (KIAA1765)
CAMK4
NDR1 (NDR)
GSK3B
GSK3A
ICK
SgK085 (LOC134927)
CHED (CDC2L5)
PITSLRE (CDC2L1)
NEK8 (AI086865)
NEK4 (STK2)
AurB (STK12)
MAK
AurC (STK13)
NuaK1 (KIAA0537)
skMLCK (MYLK2)
CRK7 (CRKRS)
CDK10
CDK7
PKG2 (PRKG2)
DNAPK/PRKDC
caMLCK (MLCK)
DAPK3
DAPK1
AMPKa2 (PRKAA2)
PIM1
PSKH1 (HUMPSKB)
CDK5
PKCt (PRKCQ)
PKN2 (PRKCL2)
PKN1 (PRKCL1)
AKT3
DMPK2 (HSMDPKIN)
IKKE
AKT1
PKG1 (PRKG1)
ATR
CDKL1
SGK2
SGK
CDKL3
CHK1 (CHEK1)
MSK1 (RPS6KA5)
ROCK1
DYRK2
CRIK (BF380737)
CDK9
BRAF
ARAF
PRKY
PAK4
NIK (MAP3K14)
DCAMKL1
PKCg (PRKCG)
CAMK2b
PKCe (PRKCE)
DCAMKL2 (BI035543)
SPEG (KIAA1297)
PINK1
PCTAIRE3
PCTAIRE1 (PCTK1)
Nuak2 (DKFZP434J037)
IKKa (CHUK)
HSER (GUCY2C)
GPRK4 (GPRK2L)
CLK3
CK2a2 (CSNK2A2)
CK2a1 (CSNK2A1)
MAPKAPK3
CAMK2g
CAMK2d
RSK4 (RPS6KA6)
PKACa (PRKACA)
PKACg (PRKACG)
Pim3 (AL549548)
p70S6K (RPS6KB1)
CAMK2a
VRK3
NEK10
MSK2 (RPS6KA4)
PKACb PRKACB
PFTAIRE2 (ALS2CR7)
SgK307
ZC2 (TNIK)
NDR2 (KIAA0965)
RAF1
SGK3 (SGKL)
PRKX
ROCK2
CK1a1 (CSNK1A1)
ZC3 (MINK)
ZC1 (MAP4K4)
CHK2 (CHEK2)
RSK3 (RPS6KA1)
PLK3 (CNK)
PLK2 (SNK)
DMPK1 (DMPK)
CAMK1g
CAMK1b
CDK4
PCTAIRE2 (PCTK2)
RSK1 (RPS6KA2)
PKCh (PRKCH)
DAPK2
ANPb (NPR2)
PKCd (PRKCD)
PKCa (PRKCA)
CDK6
RSK2 (RPS6KA3)
TAO3 (JIK)
TAO2 (PSK)
TAO1
SCYL2 (FLJ10074)
ANPa (NPR1)
PKCb (PRKCB1)
AKT2
MAPKAPK2
VACAMKL (MGC8407)
PKCz (PRKCZ)
mTOR/FRAP
RSKL2
TSSK4 (BF510751)
PRP4
PDK1 (PDPK1)
MELK (KIAA0175)
LKB1 (STK11)
HRI
HIPK4 (BG105231)
AurA (STK15)
AMPKa1 (PRKAA1)
p70S6Kb (RPS6KB2)
PFTAIRE1 (PFTK1)
IKKb (IKBKINASE)
TBK1
ZC4
MAST4 (KIAA0303)
Kinase Top List
-1
0
1
2
3
Normalized kinase statistic
Specificity Score
2
1.3
0

**Fig. S7**

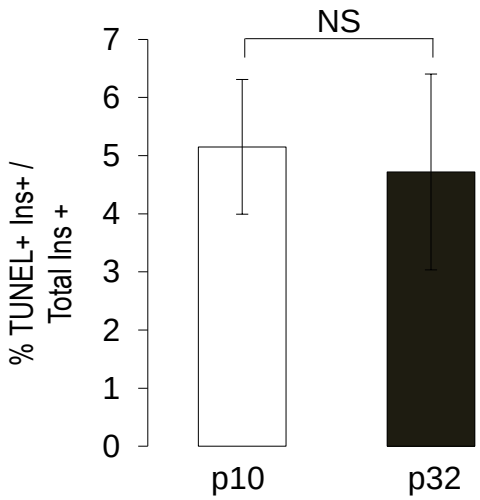

**Fig. S8**

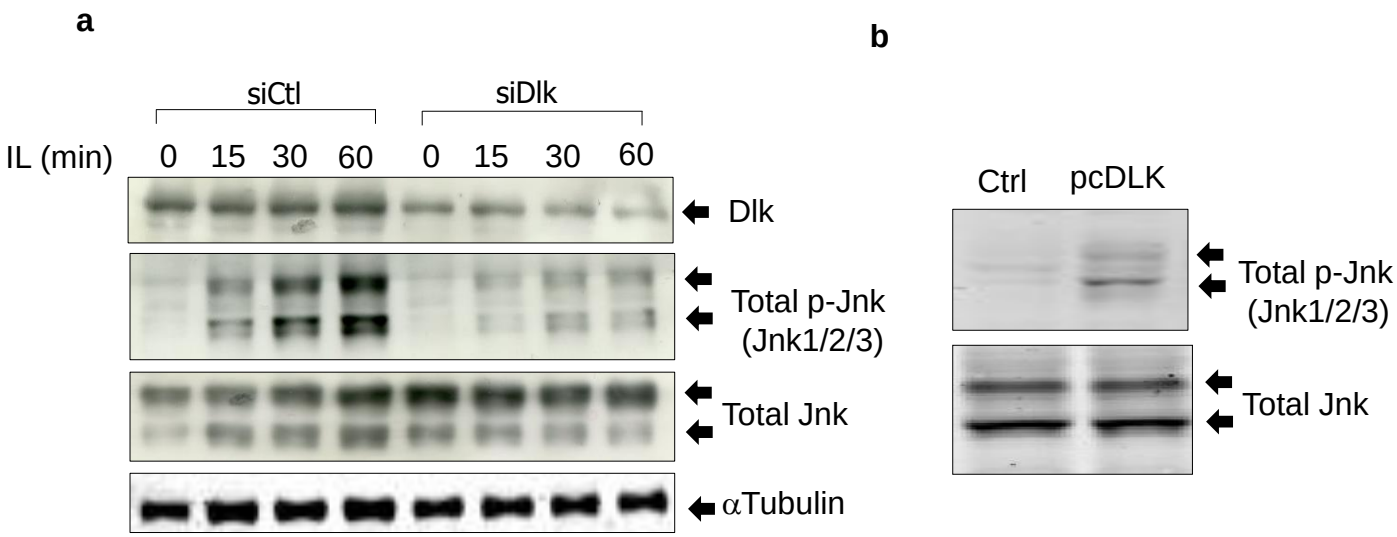
a
siCtl
siDlk
IL (min)
0
15
30
60
0
15
30
60
Dlk
Total p-Jnk
(Jnk1/2/3)
Total Jnk
αTubulin
b
Ctrl
pcDLK
Total p-Jnk
(Jnk1/2/3)
Total Jnk

**Fig. S9**

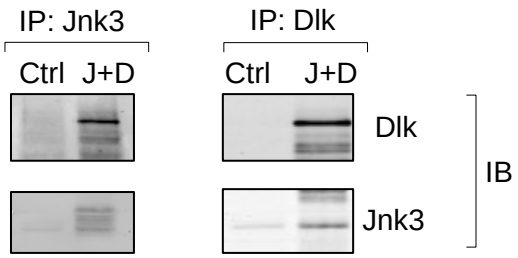

**Fig. S10**

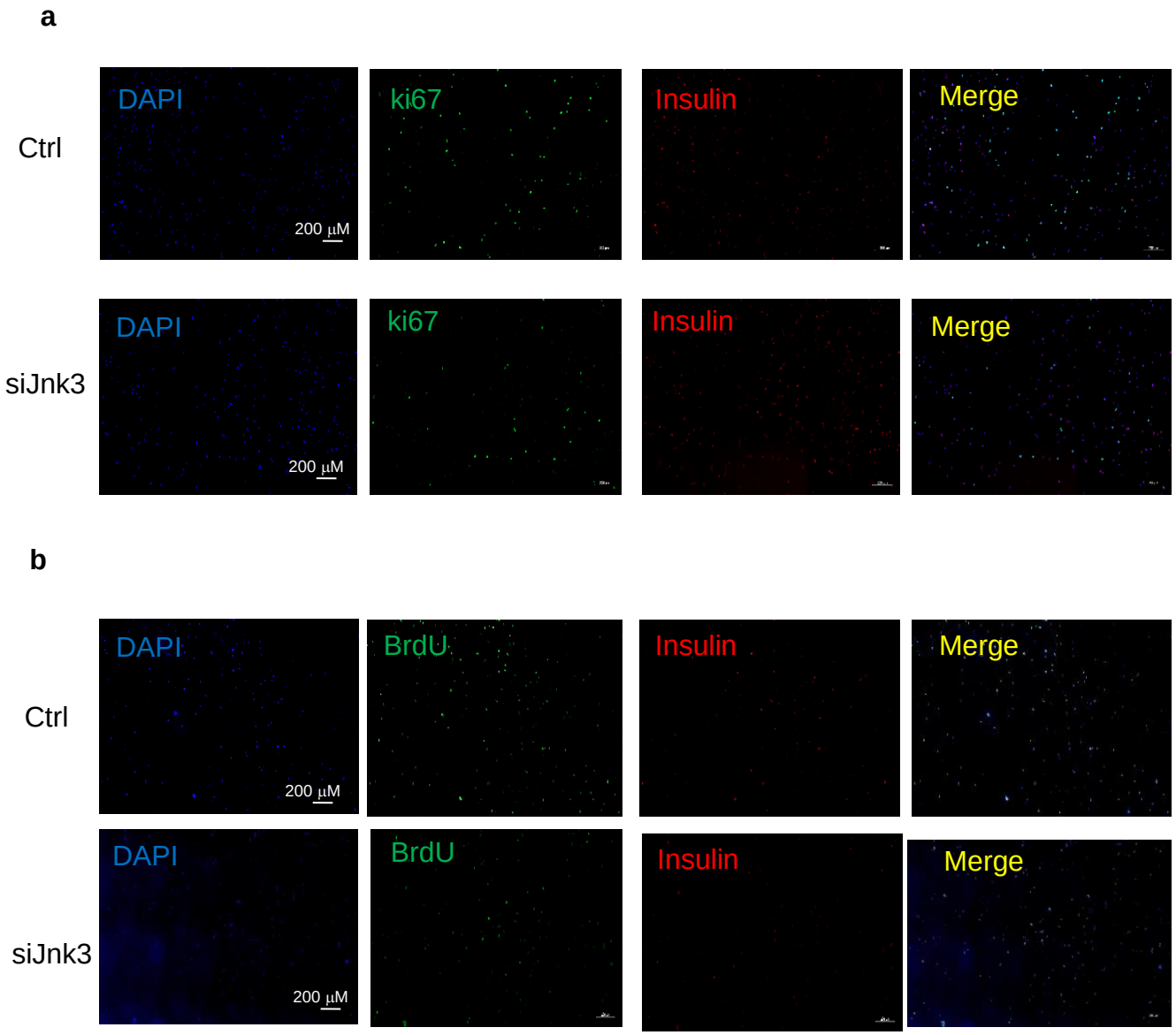
a
Ctrl
DAPI
ki67
Insulin
Merge
200 μM
siJnk3
DAPI
ki67
Insulin
Merge
200 μM
b
Ctrl
DAPI
BrdU
Insulin
Merge
200 μM
siJnk3
DAPI
BrdU
Insulin
Merge
200 μM

**Fig. S11**

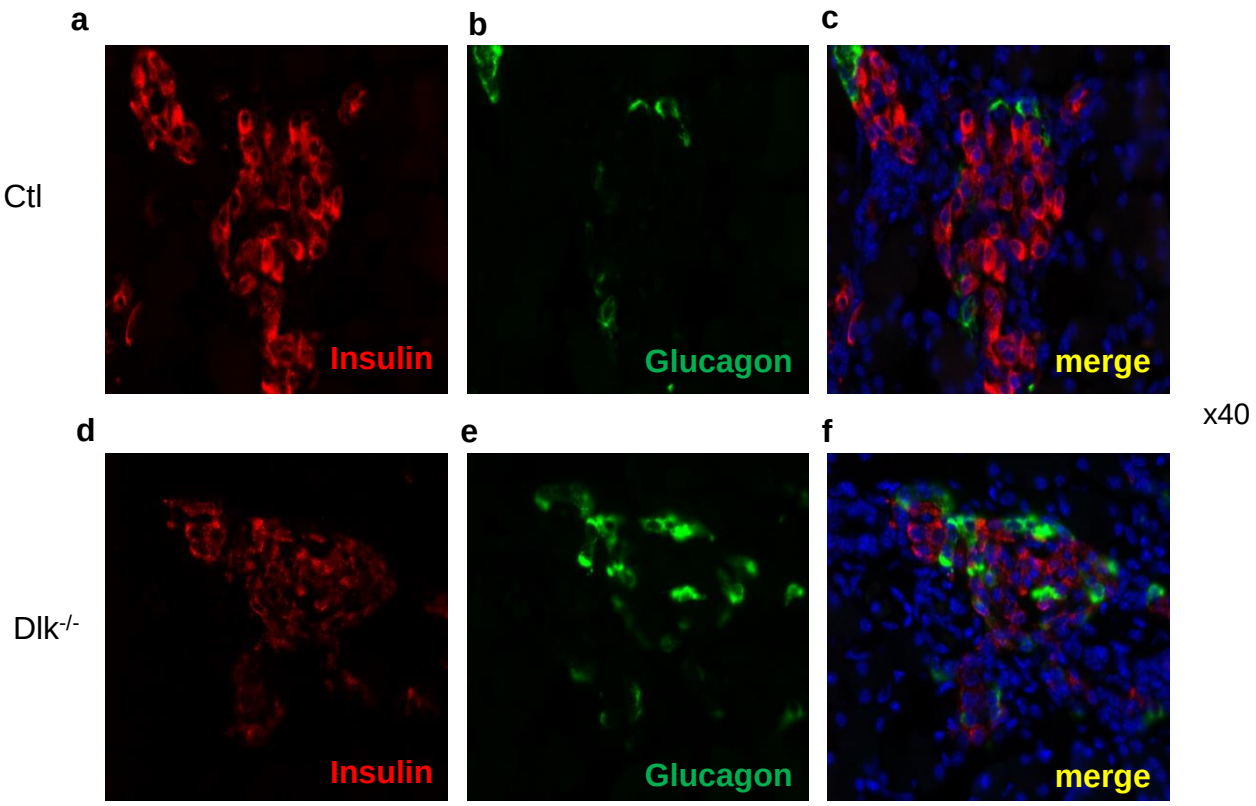
a
b
c
Ctl
Insulin
Glucagon
merge
x40
d
e
f
Dlk-/-
Insulin
Glucagon
merge

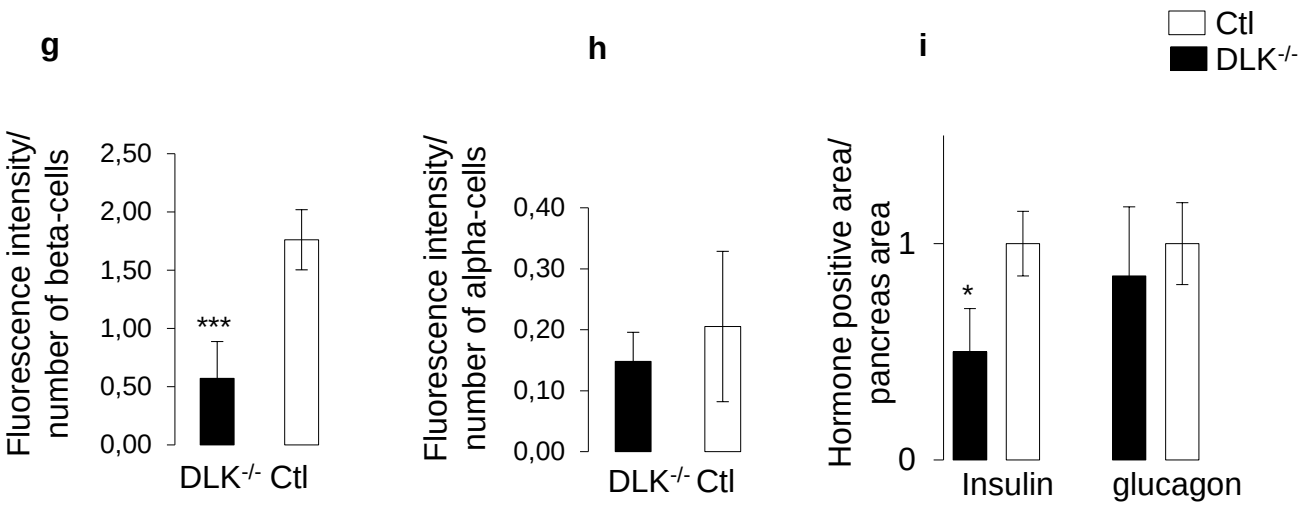
g
h
i
Ctl
DLK-/-
Fluorescence intensity/ number of beta-cells
2,50
2,00
1,50
1,00
0,50
0,00
***
DLK-/-
Ctl
Fluorescence intensity/ number of alpha-cells
0,40
0,30
0,20
0,10
0,00
DLK-/-
Ctl
Hormone positive area/ pancreas area
1
0
*
Insulin
glucagon

**Fig. S12**

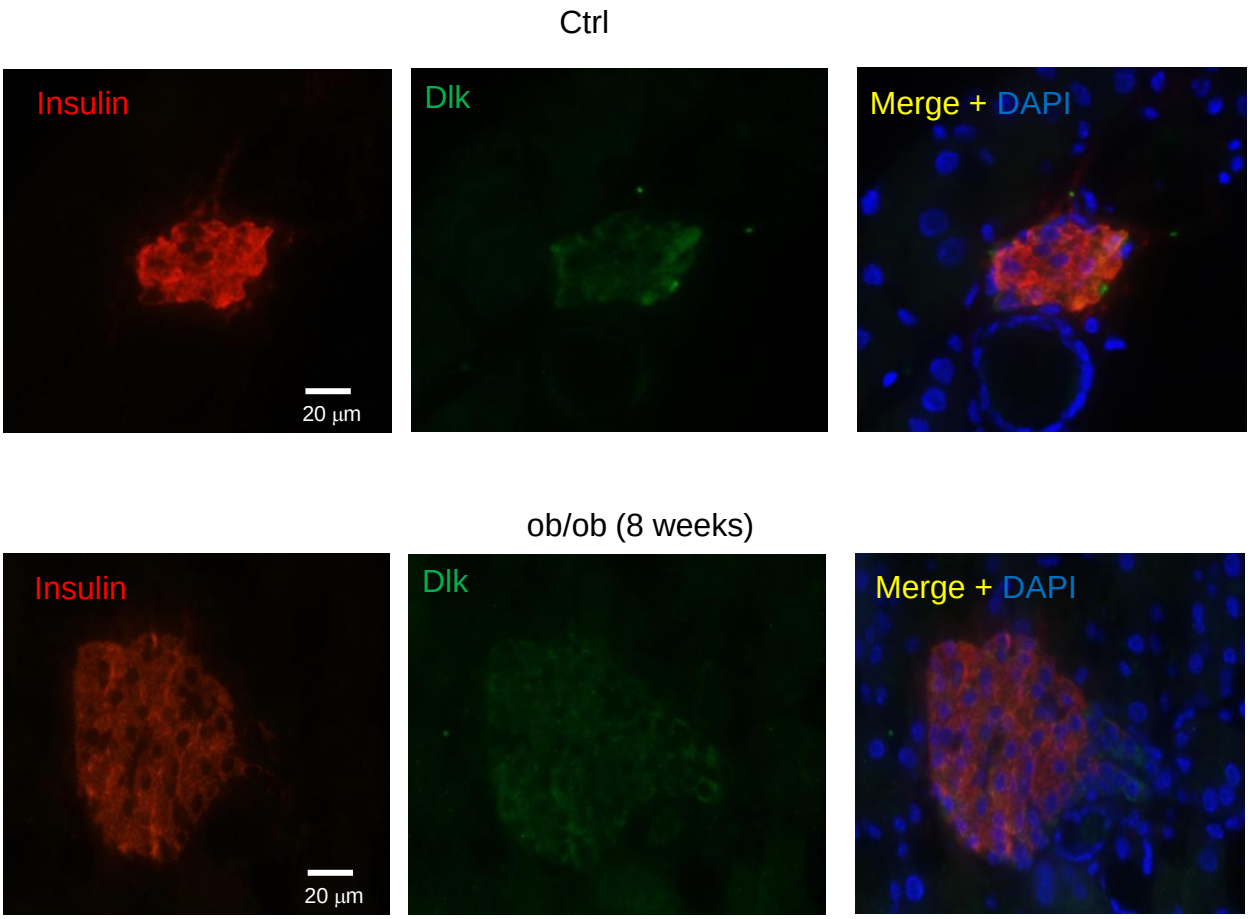
Ctrl
Insulin
Dlk
Merge + DAPI
20 μm
ob/ob (8 weeks)
Insulin
Dlk
Merge + DAPI
20 μm

**Fig. S13**

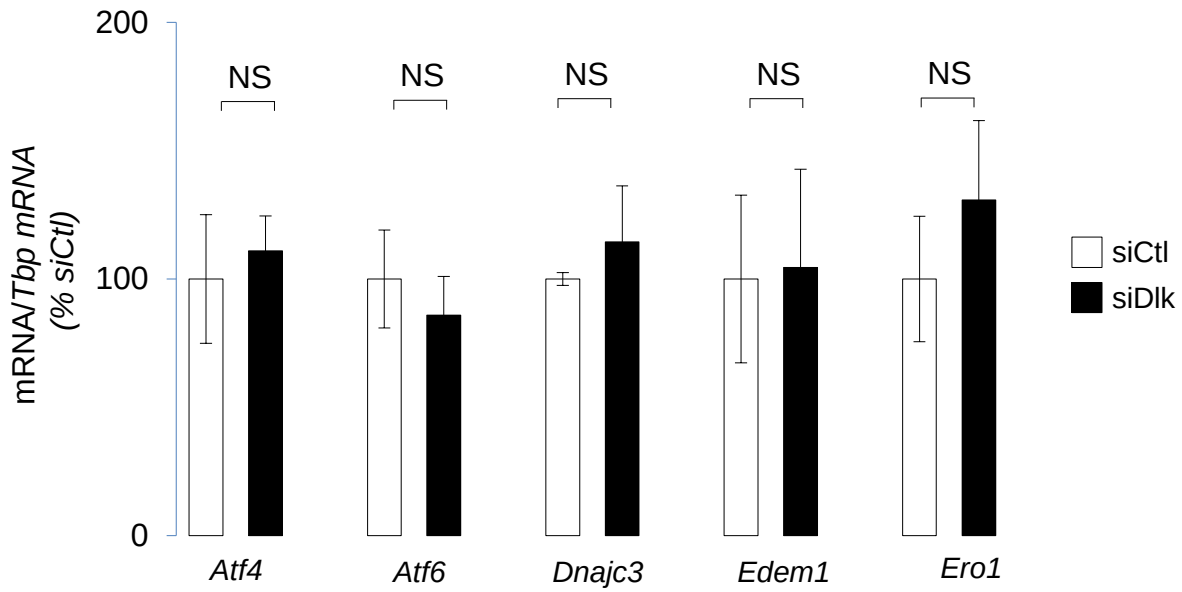
200
100
0
mRNA/Tbp mRNA
(% siCtl)
NS
NS
NS
NS
NS
Atf4
Atf6
Dnajc3
Edem1
Ero1
siCtl
siDlk

**Fig. S14**

non Diabetes

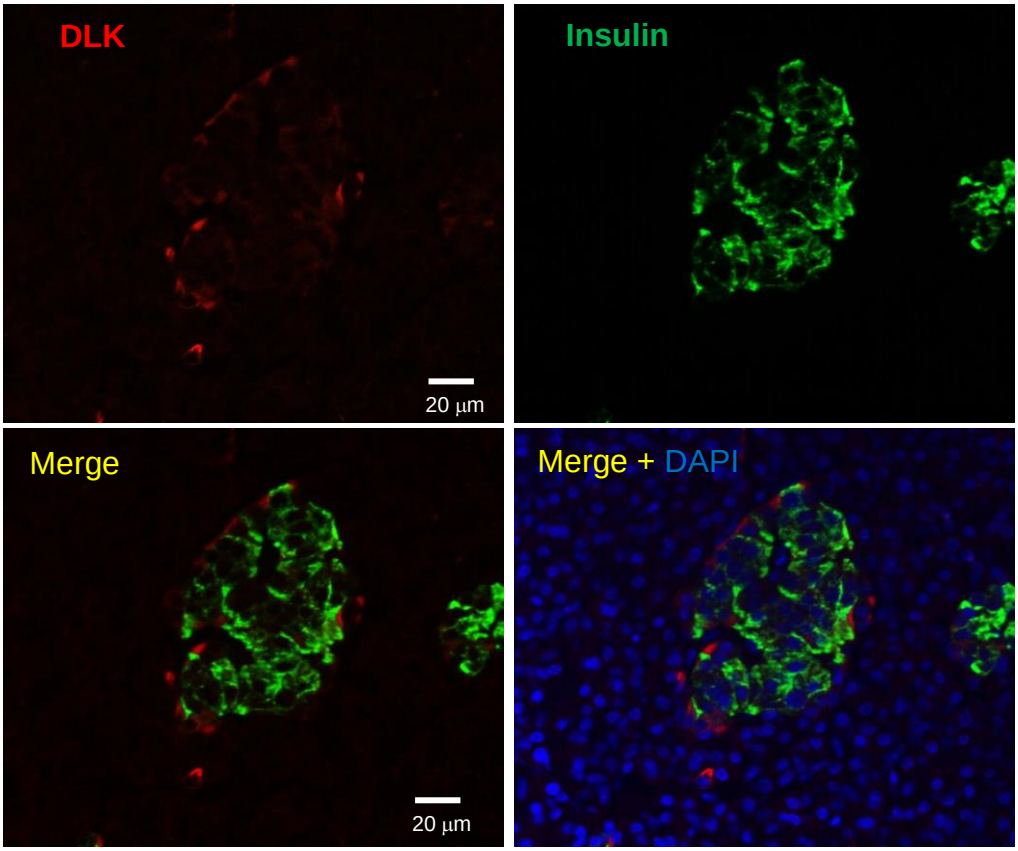


T2D patient